

Guidelines to compare additive and subtractive manufacturing approaches under the energy demand perspective

*Original*

Guidelines to compare additive and subtractive manufacturing approaches under the energy demand perspective / Ingarao, G., Priarone, P.C., Di Lorenzo, R., Settineri, L.. - In: INTERNATIONAL JOURNAL OF SUSTAINABLE MANUFACTURING. - ISSN 1742-7223. - STAMPA. - 4:2-4(2020), pp. 266-280. [10.1504/IJSM.2020.107126]

*Availability:*

This version is available at: 11583/2864872 since: 2021-01-21T17:26:45Z

*Publisher:*

Inderscience Enterprises Ltd.

*Published*

DOI:10.1504/IJSM.2020.107126

*Terms of use:*

This article is made available under terms and conditions as specified in the corresponding bibliographic description in the repository

*Publisher copyright*

GENERICO -- per es. Nature : semplice rinvio dal preprint/submitted, o postprint/AAM [ex default]

The original publication is available at <https://www.inderscienceonline.com/doi/abs/10.1504/IJSM.2020.107126> / <http://dx.doi.org/10.1504/IJSM.2020.107126>.

(Article begins on next page)

[Click here to view linked References](#)

# Structural health monitoring of historical heritage in Italy: some relevant experiences

Alessandro De Stefano<sup>1</sup>, Emiliano Matta<sup>1</sup>, Paolo Clemente<sup>2</sup>

<sup>1</sup> Department of Structural, Geotechnical and Building Engineering, Politecnico di Torino, Corso Duca degli Abruzzi 24, 10129 Turin, Italy

<sup>2</sup> ENEA, Casaccia Research Centre, Via Anguillarese 301, 00123 Rome, Italy

**Abstract.** The architectural heritage in the world represents a fundamental resource and a sign of the national cultural background. Its maintenance and preservation require a balance between the structural safety needs and the respect for their architectural and cultural value. Structural health monitoring (SHM) is increasingly emerging as a unique tool to achieve such a balance, through a proper combination of traditional and innovative techniques. This paper presents some recent experiences of SHM applied to the historical heritage in Italy, discussing relevant tools and reporting some of the most significant case studies.

**Keywords:** architectural heritage; historical constructions; structural health monitoring; masonry buildings; real case studies; damage symptoms.

## 1. Introduction

The architectural heritage represents worldwide a fundamental resource and a sign of the national cultural background. Its maintenance and preservation require a balance between the structural safety needs and the respect for their architectural and cultural value.

The largest part of the historical and architectural heritage is made of ancient masonry constructions, characterized by a wide range of uncertainties mainly due to the following reasons [1]:

- irregularity in the internal masonry texture, where lack of material, empty volumes and debris used to fill in the walls are often difficult to detect;
- imperfections related to out of plane rotations of originally vertical walls, laterally loaded by vaults, arches or roofs;
- attitude to modify in time the behavioural scheme, from monolithic elastic to cinematically articulated sets of rigid elements;
- local variability of material strength and stiffness, due to original defects, electrochemical degradation or simply the heterogeneous nature of masonry;
- distribution of cracks, increasing and reducing in length and width also according to thermal seasonal oscillation;
- effects of past, usually undocumented, damages and repairs, architectural changes and inappropriate human interventions.

The preservation of the architectural heritage is a delicate task everywhere, particularly in those countries exposed to a relevant seismic risk, like Italy.

In the lack of international standards, national guidelines have been recently issued on these topics in some countries. The relevance of structural health monitoring (SHM) as an appropriate tool to integrate and support conservation strategies is now clearly stated in the Italian National Guidelines [2]. According to the concept of “monitoring” advocated therein, local inspections are carried out as both destructive survey and non-destructive evaluation techniques in order to supply information about the structural geometry, the physical, chemical and mechanical characteristics of the masonry and of its components [3]. Such definition of “monitoring” does not correspond to the general definition contained in the first drafts of the UNI (Italian Standardization Institute) Guidelines, where “monitoring” exclusively refers to online continuous instrumented survey, excluding periodic inspections and non-destructive testing (NDT). Obviously, the artistic and historical value of ancient buildings represents a constraint for the execution of samples extractions and destructive testing. On the other side, the non-destructive survey methods can be applied only periodically and in a limited number of locations. Although useful, such survey methods supply only local information, not automatically extendable to the whole structure, and a clear understanding of the global construction behaviour is generally hindered.

As a result, multi-scale approaches based on the integration of the local investigations with global measurements should be pursued. Dynamic tests are able to provide information about the whole-body response

and the overall structural integrity [4], with some relevant limitations and drawbacks. Vibrational testing using modal parameters works well on flexible structures, like towers, vaults and domes. For example, SHM using operational modal analysis has been recently applied to two historic masonry towers, respectively built in stonework masonry and solid brick masonry [5]. In both cases simple dynamic monitoring systems (including few accelerometers and temperature sensors) were permanently installed in the upper part of the buildings to perform an automatic identification of structural modal parameters. The results allow to evaluate the effects of changing temperature on automatically identified natural frequencies and to verify the practical feasibility of damage detection methods based on natural frequencies shifts. On massive or stiff masonry bodies, on the other side, modal analysis can be subject to critical difficulties due to the crowd of local and global modes in narrow frequency ranges and to the spurious multiple harmonic components induced by the intrinsic non-linear behaviour of masonry [6, 7]. The static monitoring, on its turn, includes deformation, absolute or relative displacements, remote sensing by radar or optical scanning from ground or sky. Local inspections can reveal defects and irregularities in restricted areas, whose influence on the global behaviour would be difficult to appreciate otherwise. The availability of permanent on-line monitoring systems, able to record changes in time of the mechanical properties related to the evolution of degradation phenomena and local failures, is a fundamental requirement for the structures to become “smart”.

In what follows, some recent experiences of SHM applied to the architectural heritage in Italy will be presented. In particular, relevant tools will be discussed in Section 2 for inferring damage scenarios from structural symptoms in historical constructions, while significant Italian case studies will be reported in Section 3, distinguishing among various domains of application.

## 2. Tools for SHM of historic constructions: damage and structural symptoms

An appealing, diagnostic monitoring strategy based on the concept of “damage scenarios” has been recently proposed by Cempel [8]. A damage scenario is any anomalous operational condition for the structure induced by a specific cause and leading to damage effects that can be also difficult to detect and measure. Each damage scenario associates the causes and the consequences to a series of symptoms, i.e. physical quantities which are representative of the structural condition and can be measured by means of the appropriate sensing tools. The damage scenarios are described as functions of the observable symptoms by means of comparisons with a knowledge base or by means of numerical models of the damaged structure. The relation between damage evolution and symptoms leads to the construction of the so-called “Symptom Observation Matrix”, whose elements can be derived by the application of the conditioned probability or, more in general, the Bayesian stochastic theory [9].

Permanent monitoring systems are, as a matter of fact, symptom measuring systems. The powerfulness of an effective structural monitoring system is measured by its ability to discriminate among the symptoms, taking into account only the most significant and neglecting the irrelevant ones. Risk and reliability are probabilistic concepts. Often, in the literature, the stochastic variable is time, and the probability is the probability of time delay to the occurrence of a pre-defined damage limit state. The probabilistic distribution becomes a stochastic process in which time dependent material degradation, fatigue problems and the prediction of residual life can be easy to model and easy to combine with the risk analysis related with environmental offences, like earthquakes, floods, strong winds, landslides. The reliability of a structure,  $R(t)$ , is defined, then, as the probability that the time to reach a reference limit state,  $t_b$ , is greater than a given time  $t$  [10]:

$$R(t) = P(t \leq t_b) \quad (1)$$

The hazard function,  $h(t)$ , specifies the instantaneous rate of reliability deterioration during the infinitesimal time interval,  $\Delta t$ , assuming that integrity is guaranteed up to time  $t$ :

$$h(t) = \lim_{\Delta t \rightarrow 0} \frac{P(t_b < t + \Delta t \mid t_b \geq t)}{\Delta t} \quad (2)$$

In case of smooth time-dependent degradation phenomena,  $h(t)$  can be correlated to the reliability function,  $R(t)$ , by the following relationship:

$$R(t) = \exp\left(-\int_0^t h(x) dx\right) \quad (3)$$

1 On the other side, the hazard function allows to include into the prediction algorithm, as spikes and jumps,  
 2 also the sudden and singular events like earthquakes, floods and other environmental threats. Nevertheless,  
 3 following such path, it results not trivial to include into the risk analysis the advantages offered by the  
 4 application of on-line condition monitoring.

5 To mark the role of the on-line monitoring it is convenient to jump from the time domain into the  
 6 symptom space. The symptom hazard function,  $h(S)$ , is the reliability loss rate versus the symptom increase rate;  
 7 then reliability can be rewritten as a function of the symptom variable,  $S$ , as it is the probability that a system,  
 8 which is still able to meet the requirements for which it has been designed, displays a value of  $S$  smaller than the  
 9 value  $S_b$  corresponding to the reference limit state [11]:

$$11 \quad R(S) = P(S \leq S_b \mid S = \text{suitable value}) \quad (4)$$

$$13 \quad R(S) = \exp\left(-\int_0^S h(x) dx\right) \quad (5)$$

16 This formulation includes continuous time (slow degradation) or/and discrete time processes (earthquakes,  
 17 storms, etc.), given that time and symptom evolution can be correlated by suitable laws.

18 So, as focused above, Condition Monitoring is essentially a search for structural or material disease  
 19 symptoms. Symptoms can be regarded as evolutionary and sudden changes in observable qualitative properties  
 20 and/or measurable responses. Symptoms search can require a knowledge based direct search or model based  
 21 predictive assessment. In both cases, a stochastic procedure is needed. In some applications, direct search and  
 22 model based simulations can provide an integrated procedure.

23 In the works by Cempel (e.g. [12]) the multidimensional approach is made possible by the use of the  
 24 symptom observation matrix (SOM) and by the successive application of singular value decomposition (SVD).  
 25 On this basis, SVD allows to pass from the multidimensional-non-orthogonal symptom space to the orthogonal  
 26 generalized fault space, of much reduced dimension. Symptoms may be any measurable or observable quantity  
 27 which is sensitive to system modifications. Additionally, symptoms should be sensitive to damage evolution but  
 28 insensitive to distortions. Supposing now that  $r$  symptoms  $S_m$ ,  $m = 1, 2, \dots, r$ , are measured at  $p$  instants  $\theta_n$ ,  
 29 where  $n = 1, 2, \dots, p$ , over the system life and assuming  $p > r$ , the SOM may be defined as:

$$31 \quad O_{pr} = [S_{nm}] = [S_m(\theta_n)] \quad (6)$$

32 with  $m$  as the number of columns (symptoms) and  $n$  as the number of rows (lifetime readings).

33 The observation matrix can be a huge matrix. Singular value decomposition (SVD) can be profitably  
 34 applied to SOM in order to extract different generalized fault modes evolving in the system:

$$35 \quad O_{pr} = U_{pr} \Sigma_{rr} V_{rr}^T = \sum_{t=1}^l \sigma_t (u_t v_t^T) = \sum_{t=1}^l (O_{pr})_t \quad (7)$$

36 As a result of SVD, the symptom observation matrix  $O_{pr}$  is represented as the summation of  $l$  independent  
 37 matrices  $(O_{pr})_t$ , each describing a specific mode  $t$  of system operation modification (evolution), or generalized  
 38 fault mode. Tracing the evolution, through the lifetime  $\theta$ , of the fault modal parameters,  $\sigma_t(\theta)$ ,  $u_t(\theta)$ ,  $v_t(\theta)$  and  
 39  $(O_{pr})_t(\theta)$ , gives an understanding of the system conditions. Especially useful is the time evolution of the so-  
 40 called  $SD_t(\theta) = O_{pr}(\theta) \cdot v_t(\theta) = \sigma_t(\theta) \cdot u_t(\theta)$ , which represents a weighted summation of the symptom values for  
 41 each lifetime  $\theta$  and can be shown to give information on both the shape of a generalized fault and its energy.

42 Using both generalized fault indices  $\sigma_t(\theta)$  and  $SD_t(\theta)$ , the first related to the intensity of wear advancement  
 43 in a given fault mode and the second to its momentary shape, instead of the original symptom observations  
 44  $O_{pr}(\theta)$ , allows a more concise and powerful representation of system conditions. To better understand the  
 45 effectiveness and potential usefulness of SVD as a diagnostic tool, it is convenient, at this point, to enter more  
 46 deeply into the algorithm and to look at it from a more intuitive point of view. As stated above, we suppose that  
 47 the SOM,  $O$ , contains  $p$  observations and  $r$  symptoms, with  $p > r$  for sake of simplicity. Each singular value can  
 48 be regarded as a weighting coefficient defining the relevance of the related pair of singular vectors in  
 49 recomposing the SOM. If we choose an integer number  $s < r$ , the sum:

$$50 \quad O_{approx-s} = U_{ps} \Sigma_{ss} V_{rs}^T = \sum_{t=1}^s \sigma_t (u_t v_t^T) \quad (8)$$

51 gives the  $s^{th}$  order approximation of  $O$ , or, in other words, the reconstruction of  $O$  based on its SVD reduced  
 52 rank  $s$ . Given the choice of the reduced rank  $s$ , Eq.(8) leads to the optimal reconstruction of  $O$  among all the

1 weighted products of  $s$  pairs of orthogonal unit vectors, i.e to the minimum Frobenius norm of the matrix of  
2 residuals.

3  $\mathbf{O}_{approx-s}$  calculated by means of the first rank SVD is the optimal reconstruction of  $\mathbf{O}$  obtainable by any  
4 pair of  $x_p$  and  $y_r$  vectors, i.e. the residual matrix  $\mathbf{O}_{res-s} = \mathbf{O} - \mathbf{O}_{approx-s}$  has the minimum norm among all the  
5 possible approximations of  $\mathbf{O}$  reconstructed using any pair of unit orthogonal vectors.

6 While  $\mathbf{O}_{approx-s}$  is sensitive to the slower condition changes and progressive degradation of material and  
7 structure, the residual matrix  $\mathbf{O}_{res-s}$  is more linked with sudden or local damages. But what can be the  
8 equivalence between the wear characteristics and measures of the operating system and the SVD parameters  
9 [13]? From the physical viewpoint, different wear modes can occur like corrosion, fatigue, erosion, etc., but  
10 physically different types of wear can generate similar signals or symptoms, and there is no way of finding the  
11 expected difference in the resource of the symptom observation matrix. This means that it is of paramount  
12 importance the choice (physical origin, place of measurement, signal processing, etc.) of each observed  
13 symptom  $S_m(\theta)$  during the system operation. In general,  $\mathbf{O}$  can include heterogeneous vectors coming from  
14 various kinds of measures and observations. All the vectors shall be centered and scaled in such a way to have  
15 comparable norms.

16 If the symptoms are not correlated with damage, we will fail in getting diagnostic answers. Totally  
17 uncorrelated “symptoms”, in fact, are not symptoms at all, they are measures or observations that can have no  
18 significant links with degradation processes or localized damages. The diagnostic response will be noisy and  
19 confusing. On the other side, symptoms varying nearly in a proportional way can cause a loss of information  
20 richness. They supply all the same answer as one symptom only. The  $\mathbf{O}$  matrix will have one dimension and  
21 higher order singular values will disappear or be negligible. A good choice of symptoms shall include, for  
22 instance, observations which are sensitive to a global evolution, like, for a beam, the mid-span displacement,  
23 and other observations which are sensitive to local phenomena but correlated with the former one, like  
24 deformations or curvatures.

25 Furthermore, since in a system in operation several generalized faults may be evolving concurrently, then  
26 it is important to know also the global advancement of all generalized faults in a system.

27 Hence, some global indices are needed. It can be shown that the best choice appears to adopt the sum of  
28 absolute values of singular values:

$$30 \quad DS(\theta) = \sum_{t=1}^z |\sigma_t(\theta)|$$

33 as the measure of wear advancement, and the sum of absolute values of singular vectors:

$$34 \quad P(\theta) = \sum_{t=1}^z |SD_t(\theta)|$$

38 as the measure of the generalized fault profile.

39 Summing up, it seems possible to pass from multidimensional symptom space with high redundancy to  
40 generalized orthogonal fault space with very few generalized faults  $F_i(\theta)$ . It is also useful to create some  
41 combined measures and indices of a system condition, in terms of some norms of the symptom observation  
42 matrix, its singular values, and SVD-related summary measures and indices.

43 In [14], the authors stressed the importance of adapting the concept of the symptoms-oriented monitoring  
44 to the case of ancient masonry structures. Existing ancient civil structures are generally non-standard, unique  
45 and hardly classifiable into conventional types. At the beginning of the monitoring action, useful data and  
46 knowledge bases are seldom available. Such situation configures the phase of initial assessment of the present  
47 state. From now on, the analysis of damage evolution will move its steps. Unfortunately, the initial condition is  
48 not necessarily an undamaged condition, so its assessment shall include damage scenarios and their detection  
49 and identification.

50 The lack of real damage knowledge bases makes numerical simulation on finite element (FE) models the  
51 only practical way. If only model based simulation is available, than the damage assessment using the Symptom  
52 Observation Matrix converges to the so called “multi-model approach” to model updating.

53 Due to uncertainties and errors, each damage state can be assumed to generate infinite symptom sets, in  
54 which each symptom can change in agreement with a given probability distribution. If we use models and  
55 simulation, probabilistic procedures (including Monte Carlo search) allow generating many structural models by  
56 changing randomly material and mechanical properties; consequently, many sets of damage scenarios and  
57 symptom sets can arise.

58 The final goal is to extract damage states and their probability from the analysis of observed symptoms.

1 This kind of approach contains an implicit idea of causality. If we want to reason in terms of “conditioned  
2 probability”, instead of cause-effect, we can look at the condition monitoring using symptoms observation as a  
3 typical Bayesian problem. All model-based characterization methods belonging to the class of “multi-model”  
4 approaches can be associated to the Bayesian stochastic theory. An example of a multi-model approach to  
5 characterize an ancient masonry structure will be shown in the next section.

6 It is important to stress-out that this kind of philosophy is based on the choice of the best fitting solution  
7 among many candidates generated randomly, or determined as representative of damage scenarios, in a direct  
8 way; so the trap of the ill-conditioned nature of inverse approaches is avoided, although replaced by ambiguity  
9 (different models can fit equally well). The method is robust provided that the initial choice of damage scenarios  
10 is correct and sufficiently exhaustive [9, 15].

11 The SHM strategy can take advantage of the “multi-model” assessment technique in which a  
12 representative numerical model is not simply obtained by an optimization of the mechanical parameters of the  
13 modelled structure but by selecting the best fitting model among the many that can reproduce credible damage  
14 or defect scenarios [16, 17]. Due to the above mentioned complexity and uncertainty conditions of the  
15 mechanical nature of the historical heritage objects, it is seldom reasonable to try to design a general purpose  
16 diagnostic monitoring system. More often a previous analysis of vulnerabilities and weaknesses and of credible  
17 risk scenarios shall lead to well-focused and specifically oriented monitoring actions.

### 20 **3. Experience domains of SHM on historical constructions in Italy**

21 A non-exhaustive selection of significant SHM applications to cultural heritage structures in Italy will be  
22 presented in this section, classified on the basis of the following monitoring objectives or experience domains:

- 23 1. increasing the structural knowledge in order to assess strengthening needs and avoid unnecessary  
24 interventions;
- 25 2. verifying the effectiveness of strengthening interventions by monitoring the construction before, during  
26 and after the implementation;
- 27 3. controlling damaged structures after an hazardous event (earthquake, fire, scour, flood, etc.) in order to  
28 check the damage evolution, verify the effectiveness of provisional measures and/or help to design new  
29 interventions;
- 30 4. performing experimental analysis at fixed time intervals in order to prevent larger damage.

31 A special-case, hardly fitting in this list, will be finally proposed, regarding a laboratory investigation  
32 conducted at Turin Polytechnic on the early-warning monitoring of scouring threats in ancient masonry bridges.

#### 33 **3.1 SHM to assess strengthening needs and avoid unnecessary interventions**

34 The dome of S. Maria del Fiore in Florence, showing distributed cracks, was one of the first monitored  
35 monuments in Italy. The analysis of the first collected data did not resolve polemics on dome’s stability and on  
36 the supposed damages caused by the encircling scaffolding installed on the dome for restoration of the frescoes.  
37 In 1996 the global trend of the deformometers was traced and linked to the temperature evolution [18,19]. Blasi  
38 and Ottoni have recently presented a review of the monitoring system of Santa Maria del Fiore’s dome [20].  
39 That dome is affected by widespread crack pattern, substantially symmetric, which seems to confirm the  
40 collapse mechanism typical of the domes, with a drop of the top under its own weight.

41 Also the Flaminio Obelisk in Rome was the object of a detailed study before the restoration works.  
42 Ambient and forced vibrations were analyzed and a suitable FE model was set up also on the basis of an  
43 accurate sonic test campaign, which allowed identifying the actual damage present in the different portions of  
44 the obelisk [21].

45 Among the more recent important applications are the Roman Arena of Verona [22], the Torre dell’Aquila  
46 in Trento (where, for the first time, together with temperature sensors and long-gauge optical fiber  
47 deformometers, a network of wireless accelerometers was used [23]), the Civic bell-tower in Portogruaro [24],  
48 the San Marco and Santa Maria Gloriosa dei Frari in Venice [25], the Basilica di Massenzio in Rome (suffering  
49 from traffic-induced vibrations [26]). The long-term multi-disciplinary monitoring action on the Basilica di S.  
50 Maria di Collemaggio in L’Aquila, seriously damaged by the strong earthquake of 2009 [27], belongs also to  
51 this first objective class, rather than to the third one. Some of the most representative case studies are briefly  
52 described in the following.

##### 53 **3.1.1 The Verona Arena**

1 The Roman Arena in Verona, Italy, built in the first century A.D., is still standing in the historical city  
2 center (Fig. 1). It is open to public use for visits but also for operas, concerts and relevant shows (audience of  
3 20.000 people). It suffered damages due to aging as well as natural and man-induced events, such as  
4 earthquakes, floods, wars and sieges and, for centuries, continuative stealing of stones and material for reuse in  
5 other constructions. Past seismic events are the cause of the almost complete collapse of the third (external) ring  
6 of the monument, today only remaining in the so-called “ala” (wing) of the Arena, an isolated portion of stone  
7 blocks curved wall characterized by arches and massive pillars. Post-tensioned tendons were placed vertically  
8 along the entire height of the massive pillars in 1956.

9 With the purpose of evaluating the structural response of the Arena to static, dynamic (e.g. shows,  
10 concerts) and seismic loads, a SHM system was installed in the Arena in November 2011, with state of the art  
11 technology for data recording in relevant positions of the monument. Since no specific strengthening  
12 interventions were foreseen in the immediate future, apart from the ordinary maintenance, a SHM system  
13 installed in 2011 became an interesting tool for a strategy known as “maintenance on request”, in order to  
14 increase knowledge, reduce uncertainties and, hopefully, avoid or delay strengthening. The final aim is the  
15 acquisition of the vibration properties of the monument by means of acceleration transducers, and the control of  
16 the surveyed crack pattern through the implementation of displacement transducers installed on the main cracks.  
17 The acquired data are constantly related to the environmental parameters (temperature and relative humidity).  
18 Further details can be found in [22].  
19

### 20 **3.1.2 The Portogruaro Civic Tower**

21  
22 The Portogruaro Civic Bell-Tower is a 59 m tall, slender masonry tower, leaning with an out-of-plumb of  
23 more than 1.2 m measured immediately under the belfry. Originally built in the 13<sup>th</sup> century, it was repeatedly  
24 refurbished and its tilt was continuously monitored since 2003 [24]. The main instrument installed in it is an  
25 inclinometer, a pendulum hanging from the ceiling of the upper vault with the bottom mass damped by  
26 immersion in a water tank located at ground level to guarantee an effective damping. The position of the  
27 pendulum is permanently recorded by two digital networked cameras orthogonally oriented, which permanently  
28 acquire pictures of the wire and transmit them through the web every 10 minutes to the monitoring station,  
29 physically located at the University of Trento, where they are automatically elaborated through an image  
30 processing software. Surprisingly, the tilting imperceptible movement continues at least since 1879, which  
31 convinced the city administration to reinforce the tower foundation.  
32

### 33 **3.1.3 The Torre dell’Aquila in Trento**

34  
35 This 31 m tall medieval tower, part of the Buonconsiglio Castle, is one of the most remarkable monuments  
36 in Trento. The monitoring effort is intended to preserve the integrity of the frescoes decorating the room on the  
37 second floor, representing one of most important International Gothic artworks in Europe. The structural  
38 response is monitored since September 2008 through sensor systems, including a wireless accelerometric  
39 network and the relative development of customized hardware and software. Based on collected data, a  
40 Bayesian updating procedure allows a real-time probabilistic recognition of abnormal condition states. This first  
41 period of operation demonstrated the stability and reliability of the system, and its ability to recognize any  
42 possible occurrence of abnormal conditions that could jeopardize the integrity of the frescoes. More information  
43 are available at <http://hhms.ing.unitn.it:8080/hhms> and <http://d3s.disi.unitn.it/projects/torreaquila>.  
44

### 45 **3.1.4 S. Gaudenzio Dome in Novara**

46  
47 The dome of S.Gaudenzio Church in Novara is a 117.5 m high monument, erected between 1844 and 1880  
48 by Alessandro Antonelli, representing one of the most daring masonry structures ever built (Fig. 2). In view of  
49 its history, of past interventions and current state of preservation, this dome is representative of a broad class of  
50 problems concerning historical structures. The dome exhibited stability troubles immediately after its  
51 completion, causing an uninterrupted sequence of maintenance and strengthening interventions. In the period  
52 between 1930 and 1946, reinforced concrete was extensively used to rebuild the original upper spire; the upper  
53 part of its masonry supporting structure was encased in concrete as well; steel ties and a concrete ring were  
54 installed at the dome impost level, with the scope of preventing the collapse of the base arc.

55 A permanent static monitoring system was installed along the dome in 2000, comprising more than one  
56 hundred sensors: 52 crack displacement transducers, 16 displacement transducers, 6 load cells, 5 level gauges,  
57 one pendulum (to measure the tilt angle of the dome) and several resistive temperature detectors (RTD). The  
58 load cells, in particular, measure the tension force in the steel hoops encircling the dome at two different levels,  
59 which can be adjusted through hydraulic jacks.  
60

To record the vibrational response, the dome was also instrumented with 16 accelerometers, arranged along 4 levels (Fig. 2b). All accelerometers are directed horizontally and tangentially to the section perimeter, in order to detect torsional mode shapes too. Signals have been acquired by ambient vibration measurements, and the results of the output-only experimental dynamic identification, conducted through FDD [29], ERA [30] and TFIE [31, 32], were used to calibrate a reference FE model of the dome. The different identification techniques provided results in some cases inconsistent, which could be proved only from the comparison among different methods and with the support of a well-conceived FE model of the dome (Fig. 3). This example shows that the blind application of input-unknown techniques may result in misleading conclusions in the case of very complex structural works. Indeed, no method is capable of providing information that is not contained in the signal, independently on how refined the method can be. Table 1 shows the comparison among the different estimation sources [28]. Some interesting intervention proposals were also formulated [33].

**Table 1** S. Gaudenzio Dome in Novara - Modal shapes and frequencies using different identification techniques

Modal shape recognition		Frequencies [Hz]			
		FEM	ERA	FDD	TFIE
1 <sup>st</sup> bending	(along x)	0.82	0.75	0.79	0.79
	(along y)	0.82	-	0.81	0.82
2 <sup>nd</sup> bending	(along x)	1.45	1.70	1.63	1.62
	(along y)	1.45	-	1.67	1.68
1 <sup>st</sup> torsional	-	1.64	-	1.73	1.74
3 <sup>th</sup> bending	(along x)	2.64	2.42	2.63	-
	(along y)	2.64	-	-	-
2 <sup>nd</sup> torsional	-	2.99	-	-	-

### 3.1.5 The Sanctuary of Vicoforte

With its internal axes of about 37.2 m by 24.9 m, the dome of the Sanctuary of Vicoforte, North-West Italy, is the fifth biggest in the world in absolute terms, and by far the largest elliptical dome ever built. The duke Carlo Emanuele I Savoia committed to the architect Ascanio Vitozzi the design of the Sanctuary in 1596, to make it a site of pilgrimage and a mausoleum for the Savoia family (later the Italian royal family from 1860 to 1946), but the huge construction was completed only in 1731 (Fig. 4).

The Sanctuary, a bold, highly prestigious, structure, underwent retrofits and modifications during all of its life and suffered significant damages. Recently, a nonlinear model was used to simulate the whole structure-foundation-soil system behaviour, accounting for the presence of deep layers of soft soil under the building, allowing significant settlements over the years and potentially causing serious damages in case of strong seismic actions [34]. The monument has been recently chosen as a case study for the evaluation and application of the Directive PCM 2008, describing the procedures to be followed in assessing the safety of an existing building [2]. For architectural heritage, this must be done in several steps: a) identification of the structure; b) geometric data gathering; c) historical analysis; d) survey of the materials and their state of preservation; e) mechanical characterization of the materials; f) soil and foundation analysis; g) monitoring. The first basic steps, including NDT, characterization of masonry and foundation soil and description of the geometric data and crack patterns, had already be concluded previously together with a general plan of future investigations [34]. Further studies were dedicated to the vibrational response and modal characterization. Due to the complexity and large size of the building, the experimental campaign focused on the dome, whereas for a seismic assessment the main interest rests in global modes, especially those falling in a low frequency range [35], and in the long-time measure of the deformation stability of the metal ties fastening the base of the dome [36].

The data acquisition campaign at the Sanctuary of Vicoforte was performed in June 2008 using four triaxial geophones with a sensitivity of 400 V/m/s and 5 accelerometers with 10 V/g sensitivity, relocated according to different setups so as to obtain a reliable global identification of the structure. The accelerometric signals were sampled at 128 Hz. All recorded signals were conditioned using filters, de-trending and subsampling. Signals were segmented in overlapping time windows and statistically treated. Computational modes were systematically discarded by using modal assurance criteria [37]. In more detail, all signals coming from different acquisitions were segmented and a great number of stochastic subspace identification (SSI) [38] sessions were performed. Stabilization processes were used to exclude apparent modes with too low energy to be surely recognized as true modes and probably due to exogenous components. Three real modes were finally identified, having frequencies equal to, respectively, 1.99 Hz (along-y, 1<sup>st</sup> bending mode), 2.08 Hz (along-x, 2<sup>nd</sup> bending mode), 3.42 Hz (torsional mode).

The FE model was built, using solid 8-node elements, as a predictive tool focused on the slow soil settlement and the crack it had already caused and will possibly still cause to the dome (Fig. 5). The model is complex and large, cast with the aim to manage non-linear analyses, keeping account of the soil-structure static interaction but with the usual simplified assumption that masonry is an isotropic homogeneous material. A basic linear version, neglecting the dynamic soil-structure interaction, was used to perform a very simple and rough model-updating, just to assess on an experimental basis the average values of the Young modulus and Poisson ratio at the initial quasi-linear small deformation stage. The updating process used the classical minimum error strategy comparing the experimental and computed values of the two first bending modes in the x and y directions (the symmetric shape of the monument allowed to clearly separate translational and torsional modes).

Table 2 shows the evolution of the two average parameters in the model and the reference experimental values. It shows also the dramatic problem of the huge uncertainties in the assessment of the mechanical properties of many ancient masonry structures, underlined by the huge scattering of the experimental estimation of the Young modulus. The use of global average values could hide unexpected local vulnerabilities although, in this case, the reduced set of updatable parameters is due to the size and complexity of the model and, anyway, the symmetric vibrational behaviour supports somehow that choice. The predictive capacity of the model required a sophisticated and complex modeling. It was important to create a consistent initial condition state description, using NDT tests and precise geometric assessment of the structural shape and existing visible damages. The building is a massive construction, whose dynamic characterization is difficult because of the intrinsic non-linearity and closeness of the modal frequencies. The drawback of the numerical accuracy is the limited number of parameters reliably usable to update the model.

**Table 2** The Sanctuary of Vicoforte - Updated parameters of the FE model

Property	First attempt value	Updated value	NDT value (2004)
Elastic modulus E (MPa)	1635	2330	1300-4800
Poisson's ratio $\nu$	0.4	0.38	0.39

### 3.1.6 The Ghirlandina Tower in Modena

The case study of the Ghirlandina bell-tower is important for its general implications [39]. The wonderful Cathedral of Modena (central-northern Italy) and its bell-tower Ghirlandina are part of the UNESCO site Piazza Grande (Fig. 6). The construction of the tower began in 1099 together with the cathedral and ended in 1319. The arches connecting the southern side of the tower to the cathedral were set in place in 1338, because there was evidence that a tilt, later corrected, occurred during the construction. Measurements of the tilt and studies on the foundation depth and consistency started at the end of the nineteenth century. In 2007 a scientific committee found that the brick-made foundation had a thickness of 3 m and was conceived as a spread foundation without supporting piles. It was possible to define the settlement suffered by the tower ( $\sim 2$  m) and the compressibility of the foundation soil. Over the last decade, there has been a growing interest in the potential seismic vulnerability of the tower and its interaction with the cathedral. This interest was further increased by the recent earthquake in the Emilia Romagna region in May 2012 because many historical masonry bell towers collapsed despite the moderate magnitude ( $M = 5.9$ ) of the seismic event.

Strain-hardening plasticity models, the so-called macro-element models of the overall soil-footing systems, are accepted as providing reliable simulations [40]. Ambient vibration tests and identification supplied significant contributions [41]. A model updating procedure is needed to build a reliable predictive tool [42]. Models of ancient towers founded on soft soil must include soil-structure interaction, otherwise no updating leads to reasonable results. The soil profile down to the investigated depth of 80 m is a sequence of recently deposited alluvial horizons; medium- to high-plasticity inorganic clays are surmounted by 5-7 m of alluvium linked to flooding events (of post-Roman era) produced by minor streams. Cross-hole tests revealed a shear wave velocity (VS) ranging from 100 to 200 m/s in the upper 20 m, more dispersed values, up to 500 m/s, from 20 to 35 m deep, about 200 m/s below 34 m.

Ambient vibration tests were used to estimate the modal parameters of the tower. Ten triaxial accelerometers, having 1 V/g sensitivity and  $\pm 5$  g measure range, were installed on the tower to record the time histories located on the base of a preliminary FE analysis on a model composed by some thousands of iso-parametric solid or Mindlin-Reissner shell elements or truss elements to simulate constraints and sub-soil deformability.

Soil-foundation interaction, mechanical properties of masonry, changes of geometry along the vertical axis and the arches linking the tower and the cathedral body are all conditions influencing more or less significantly the analysis results. The analysis of sensitivity of mode shapes to these parameters allowed to avoid ambiguous

estimates due to spatial aliasing [43]. The dynamic parameters of the structure were identified in the time domain using the SSI method, separately in horizontal and vertical directions.

The selection of frequencies of vibration and the corresponding mode shapes was made on the basis of the recurrent forms, with an equivalent viscous damping less than 10% and a level of affinity higher than 90%, evaluated by means of the MAC [37] (Table 3).

**Table 3** The Ghirlandina Tower in Modena – Frequency and damping of the 9 identified modes

Mode	Frequency Hz	Damping %	Mode	Frequency Hz	Damping %
1	0.74	1.43	6	4.81	2.77
2	0.85	1.24	7	5.25	1.66
3	2.77	2.47	8	4.51	7.36
4	2.99	4.01	9	9.79	7.95
5	3.66	3.76			

Results show that soil-structure interaction cannot be neglected, in contrast to most published identification analyses on ancient towers, which usually assume the structure to have rigid constraint at its base. In fact, the first bending mode-shape as well as mode-shapes related to vibrations along the tower axis (modes 8 and 9) with associated frequencies of 0.74, 4.51, and 9.81 Hz, respectively, showed that the rotation and displacement pattern at the tower base was mainly due to soil deformability [44]. Optimized values for the masonry Young modulus range from 3 to 4 GPa.

In order to assess the safety condition with respect to a specified limit state or to evaluate the seismic response of the structure, tracing the local response spectra coherent with the expected ground motion at different levels of the tower, the use of an updated FE model is needed. The model updating procedure adopted in this case-study is the inverse eigensensitivity method (IESM), based on the properties of the initial system and on the first-order sensitivity functions of these properties [45, 46]. The parameters updated in the optimization analysis are the masonry elastic modulus of the 11 segments of the tower, the stiffness of the 8 truss elements representing the arches and the vertical and horizontal stiffness of the soil-foundation system.

After the updating process, using the complete set of modal data, the maximum error between the experimental and numerical modal parameters decreased to a little more than 2% of the lower value. The significance and quality of the results and the rigorous and up-to-date methods and model assumptions make this research really outstanding.

### 3.1.7 The Duomo of Orvieto

The Duomo of Orvieto is a Gothic-Romanesque style church, built between 1290 and 1320. The very famous facade is a mix of marble and mosaics. It has a 17 m wide nave and two 8.5 m wide aisles. The 59 m long nave is covered by a wooden truss roof, supported by masonry walls. Each wall is supported by six arches stemming from circular masonry pillars, which separate the nave from each aisle. The Duomo was interested by the 1997 Umbria-Marche seismic crisis. Three main shocks were recorded on September 26<sup>th</sup>, the first at 2:33 a.m. (Italian time,  $M_L=5.5$ ), the other two at 11:40 ( $M_L=5.8$ ) and 11:46 a.m. ( $M_L=4.7$ ). The epicentral area was at about 70 km far from Orvieto. The first shocks caused the opening of cracks in the structures, and ENEA was involved in the experimental analysis of the structural behaviour, in order to evaluate the health status of the building and to locate any damage. The structures of the Corporale's Chapel were particularly studied [47].

The structure showed a good performance both in the ambient vibration and forced tests (Fig. 7). The velocity amplitude due to ambient vibrations was very low if compared to that obtained in other cases or suggested as allowable ones. The analysis of the recorded data relative to ambient vibration tests allowed identifying the resonance frequencies of the structure. The behaviour of the vaults was also analyzed by means of forced vibrations. The main structure of the nave showed a good performance, even though there was no rigid connection between the longitudinal walls. Horizontal constrains between the wooden roof and the masonry walls are missing. Several structural resonance frequencies related to different modal shapes were identified.

Forced tests of the vaults showed resonance frequencies slightly different from those pointed out by ambient vibration tests. More significant differences were observed in the records obtained on the vaults of the choir and on that of the transept during earthquakes, probably due to the mechanical non-linearity of masonry. The presence of some cracks in the vaults also played an important role.

### 3.1.8 The Lateran Obelisk in Rome

The Egyptian Lateran Obelisk was the object of restoration works between 2007 and 2008. As a preliminary step, a comprehensive structural health analysis was carried out, including ambient vibration tests,

1 sonic and radar measurements [48, 49]. The obelisk is 32.2 m tall and rests on a rectangular prismatic pedestal,  
2 about 10 m tall, which in turn is placed on a wide stone basement, whose depth is not known as well as the  
3 foundation conditions. A Christian cross is at its apex, so the total height is 45.7 m. The Obelisk itself is made of  
4 three monolithic tapered red granite blocks, which exhibit various cracks particularly visible near the contact  
5 surfaces between the blocks. Externally visible metallic links and small pieces of granite added during past  
6 restorations connect the blocks to each other.

7 The experimental analysis was carried out by a temporary seismometric array (Fig. 8a). Several  
8 measurements were carried out. Traffic-induced vibrations of various intensities were recorded during the day,  
9 as well as ambient noise vibrations during the night. The choice of the sensor locations was influenced by their  
10 accessibility and the presence of a plane surface.

11 For all the recordings, time domain and frequency domain analyses were carried out. Resonance  
12 frequencies were identified close to 1.27 Hz, for both the N-S and W-E first bending modes. The third and the  
13 fourth modes, in the N-S and W-E directions, were associated to frequencies equal to 6.15 Hz and 6.73 Hz,  
14 respectively. Modal shapes are plotted in Fig. 8b. No significant amplification effect were pointed out by the  
15 HVSR, on the other hand a peculiar behaviour was observed at frequencies above 8 Hz, where the spectral  
16 amplitudes of the vertical components of motion appear remarkably higher than those of the horizontal  
17 components. This effect could be related to caves and ancient structures that are known to be buried below the  
18 ground level.

19 The FE model was set up by using solid elements. The model was composed of four regions characterized  
20 by homogeneous material properties. Their weights per unit volume were fixed according to the well-known  
21 values derived from the literature, while their Young's modules were automatically updated in order for the  
22 numerical first frequency and modal shape to reproduce the experimental ones. It is worth pointing out that, the  
23 geometry of the foundation being unknown, also the height of the basement was changed in order to reproduce  
24 the horizontal displacement on the basement.

25 The updated model was used for the non-linear static analysis. Between the basement and the pedestal, and  
26 also between the pedestal and the Obelisk, no-tensile resistant gap elements were introduced in the model. The  
27 structure was subjected to its self-weight and to an increasing horizontal load distribution reproducing the  
28 effects of the first modal shape. In Fig. 8c the resulting diagram of the acceleration versus the displacement at  
29 the top of the Obelisk (pushover capacity curve) is plotted. The loss of stability is apparent for very low values  
30 of acceleration, the large displacement being mainly related to the relative rotation between the Obelisk and the  
31 pedestal.

### 34 **3.2 SHM to verify the effectiveness of strengthening interventions**

36 SHM can be very useful to validate the effectiveness of structural interventions by experimental analyses  
37 before, during and after the implementation.

38 This is the case of the Cansignorio stone tomb in Verona and the case of S. Sofia Church in Padua [50,  
39 51]. Let's mention also the outstanding stabilization and monitoring work on the leaning tower in Pisa [52].  
40 Another recent application of SHM to architectural heritage buildings is proposed by Del Grosso *et al.* [53] in  
41 the Royal Villa of Monza, suffering from foundation settlement: a monitoring system was installed to control its  
42 movement before and during the refurbishment works and the subsequent service life, with a relevant use of  
43 fiber-optic sensors. An interesting study was carried out on the Marchesale Palace in San Giuliano di Puglia,  
44 damaged by the 2002 Molise earthquake, both before and after the retrofit intervention [54].

45 Ambient vibration analyses were carried out on the Round Temple at the Forum Boarium, before and after  
46 the structural interventions on the columns and the covering, to assess their effectiveness [55, 56].

#### 48 **3.2.1 Cansignorio Stone Tomb**

49 The Scaliger Tombs is a group of five Gothic funerary monuments in Verona, Italy, celebrating the  
50 Scaligeri family, who ruled Verona from the 13<sup>th</sup> to the late 14<sup>th</sup> century. Throughout the centuries, several  
51 repair interventions were necessary to preserve the delicate structure of the stone tomb, such as those carried out  
52 in the XVII, XIX and XX centuries (Fig. 9a and 9b).

53 Having activated a SHM system before, during and after interventions allows in fact the application of the  
54 so-called incremental approach, which means intervening following a step-by-step procedure, checking  
55 continuously the system response and modifying, if necessary, the intervention strategy according to the  
56 outcomes of monitoring [50]. Between 2006 and 2008, a light strengthening intervention at local and global  
57 level improved the structural and seismic capacity of the monument, stabilized some critical points and repaired  
58 deteriorated parts or elements [51].

1 At the global level of structural members the proposed interventions aimed at the enhancement and  
2 upgrading of the existing hooping and confinement system by means of the insertion of high-strength steel  
3 cables in addition to the existing iron tie rods.

4 At a local level two main interventions were performed:

- 5 • Application of CFRP strips to repair the deteriorated parts of the equestrian statue: this reinforcement is  
6 made of carbon fibres impregnated in a polymeric matrix;
- 7 • Confinement of a cracked capitol by means of the application of a hooping system composed by high-  
8 strength steel cables ( $\varnothing$  1.6 mm).

9 For the identification of the modal parameters (natural frequencies and corresponding mode-shapes),  
10 output only identification techniques (FDD) were used.

11 The sensing system (installed in December 2006) controls the static and dynamic structural performance  
12 and the effectiveness of the adopted strengthening solutions.

13 It is composed by (Fig. 9c):

- 14 • 1 acquisition unit;
- 15 • 6 high sensitive single-axis piezoelectric accelerometers;
- 16 • 2 potentiometric displacement transducers;
- 17 • 1 temperature and relative humidity sensor.

18 The central unit, located at the base of the tomb, is provided with a Wi-Fi router for remote data  
19 transmission. For details and outcomes see [50, 51]. The most relevant aspect of the Cansignorio tomb  
20 monitoring is not in the results themselves but mainly in the “design by testing” and “retrofit by testing”  
21 strategy, often adopted in the world of historical heritage, due to the large amount of uncertainties, but seldom  
22 practiced like here as a declared and systematic procedural choice.

### 23 **3.2.2 The medieval Bell Tower of S. Giorgio in Trignano**

24 The medieval Bell Tower of S. Giorgio Church in Trignano, 18.5 m tall and 3.35 m by 3.00 m at the  
25 basement, withstood several changes and additions in the past centuries. Four masonry pillars at the corners,  
26 about 40 cm thick, compose the main structure. Very poor masonry walls, whose connections with the pillars  
27 are not effective, fill the spaces between the pillars. The first three floors were made of timber, the fourth one had  
28 been substituted by a two brick little vault floor, supported by a central steel I-beam. The stairs were composed  
29 by wooden and steel flights. The tower is connected to the structure of the church and to other masonry  
30 buildings on three sides, up to the height between 6 and 7 m. It was seriously damaged by the Reggio Emilia  
31 Earthquake ( $M_L = 4.8$ ) on October 15<sup>th</sup>, 1996. The most apparent effect of the earthquake was the opening of a  
32 near horizontal crack in the freely rising part, above the roofs of the adjacent buildings. The crack interested  
33 three of the four sides of the tower. A 3 cm offset was also apparent between the upper and the lower part of the  
34 East wall, due to a clockwise rotation of the upper part with respect to the lower one.

35 A preliminary dynamic characterization was first performed just after the seismic event [58]. Then six  
36 accelerometers were installed and sixty-seven low magnitude aftershocks were recorded in about two months  
37 [59]. The dynamic characterization of the tower was performed by means of ambient vibration tests. Also  
38 vibrations due to the effects of a mass dropped on the ground near the tower were recorded. The motion in terms  
39 of modal shapes was examined by means of the power spectral densities (PSD) amplitudes. The ambient  
40 vibration tests showed a resonant frequency of about 2.7 Hz with prevalent displacements in the N-S direction,  
41 and a resonant frequency of about 2.9 Hz with prevalent displacements in the W-E direction. A resonant  
42 frequency of 6.9 Hz was associated to a torsional modal shape.

43 The fixed instrumentation consisted of a triaxial accelerometric sensor located on the ground floor, which  
44 could be assumed as basement, and three uniaxial horizontal accelerometric sensors at the top (Fig. 10a). The  
45 sixty-seven aftershocks recorded were classified on the basis of the input energy for the structure, estimated by  
46 means of the Arias scalar intensity at the basement ( $I_A$ ). The records obtained under the lower energy  
47 earthquakes confirmed the results of the dynamic characterization. The dynamic characteristics, in terms of  
48 resonance frequencies, modal shapes and damping, significantly changed under earthquakes of higher level  
49 energy. The first frequencies were equal to 2.25, 2.60 and 5.50 Hz and were associated to modal shapes with  
50 prevalent displacements in the N-S direction, with prevalent displacements in the W-E direction and to a  
51 torsional movement of the tower, respectively.

52 The frequency domain analysis was performed for all the events. Changes in the resonant frequencies for  
53 different seismic intensities were apparent (Fig. 10b). For low Arias intensities, the resonance frequencies were  
54 almost independent of the seismic energy and very close to those obtained from the characterization tests. For  
55 larger intensities, all the three resonance frequencies decreased almost linearly with  $\text{Log}(I_A)$ . For each of the  
56 three frequencies, the threshold between the two intervals equals  $I_{A,0} \approx 5 \cdot 10^{-4}$  cm/s, which was assumed as the  
57 limit value for the seismic energy separating the range of the linear behaviour of the damaged tower from the  
58

1 non-linear range. The coherence function assumed lower values for the strongest earthquakes, as a result of the  
2 nonlinear seismic behaviour of the tower. In some cases, a different behaviour appeared under earthquakes of  
3 similar amplitude, likely a consequence of the variable directivity of the earthquakes. Damping, calculated by  
4 means of the half power bandwidth method, increased with the energy level. The reduction of the first resonance  
5 frequency and the increase of damping clearly resulted from the transfer functions in Fig. 10c. The tower was  
6 finally restored by using shape memory alloy (SMA) devices [60].

### 7 8 **3.2.3 The Hospital in Pievepelago** 9

10 The Pievepelago Hospital was built at the beginning of the 20<sup>th</sup> century. Before the intervention it was  
11 composed of a main rectangular building and two adjacent smaller structures (dashed line in Fig. 11). The  
12 carrying structure of the main building was formed by two right-angled sets of masonry walls, whose health  
13 status seemed to be quite good. Some existing cracks could have been caused by the 1983 earthquake. The  
14 building still had the original wooden floors at the garret (fourth floor) and the roof. The second and third floors  
15 had been replaced with iron floors in 1955. The horizontal structure was missing at the ground floor (first floor).  
16 The existing floors could not be considered as rigid diaphragms between the walls, due to their flexibility and to  
17 the absence of an effective connection with the walls. A real foundation structure was missing. The masonry  
18 walls were fitted in the ground for about 2 m.

19 The structural strengthening consisted in the demolition of the smaller structures and in the construction of  
20 a reinforced concrete tower to contain the lift. A seismic joint between the new structure and the old building  
21 should guarantee the absence of any dynamic interaction between them. The third floor and the old roof were  
22 replaced with a new floor and a new roof made of reinforced concrete with bricks. The first and the second steel  
23 floors were strengthened by means of a reinforced concrete slab of 5 cm thickness. A reinforced concrete slab  
24 was also cast on the first (ground) floor, in order to join the walls at this level.

25 In the first experimental campaign on the existing building, six seismometers and two recorders Lennartz  
26 MARS-88 with three channels were used [61]. The dynamic load was produced by using a lorry and a steam-  
27 roller moving at the same time along one or two sides of the building (W and S). The case of only noise input  
28 was also considered. Several tests were performed deploying the seismometers in different configurations. Data  
29 analysis consisted in frequency domain analysis. Three frequencies were identified as structural resonances:  $f_1 =$   
30 4.4 Hz (bending in the N-S direction),  $f_2 = 5.0$  Hz (bending in W-E direction),  $f_3 = 6.4$  Hz (torsion). The  
31 connections between the walls were effective, except for those between the main building and the adjacent  
32 smaller ones. The structural vulnerability was essentially related to the absence of horizontal rigid diaphragms,  
33 necessary to guarantee a suitable distribution of the seismic actions.

34 A detailed experimental analysis was carried out after the structural intervention [62]. The following  
35 resonance frequencies were obtained:  $f_1 = 5.7$  Hz,  $f_2 = 6.2$  Hz and  $f_3 = 8.4$  Hz, corresponding to the previous  
36 ones, respectively. A fixed accelerometric network was installed by the National Seismic Survey, which  
37 recorded the first seismic event on December 24th, 1997, just after the completion of the works.  
38  
39

## 40 **3.3 SHM to control damaged structures after a hazardous event** 41

42 SHM can be used to check the evolution of damages and verify the effectiveness of provisional  
43 strengthening measures or to help to design new interventions.

44 More than one team monitored the Civic Tower and Palazzo Margherita in L'Aquila [51, 63]. The work  
45 described in [63] will be shortly presented, as well as the monitoring project for the Holy Shroud Chapel in  
46 Turin [17, 64, 65]. Many other applications to buildings which were severely damaged after L'Aquila  
47 earthquake deserve mentioning: Anime Sante, S. Marco, S. Biagio, S. Giuseppe, S. Agostino, S. Silvestro  
48 Churches, the Spanish Fortress [51, 66]. The already mentioned Bell Tower of S. Giorgio Church in Trignano,  
49 damaged by the 1996 Reggio Emilia earthquake, was monitored by means of an accelerometric network for  
50 about two months, which allowed analyzing the actual behaviour under earthquakes of different energy and  
51 detecting any damage increase. The same procedure was applied to the CEDRAV building in Cerreto di Spoleto  
52 after the 1997 Umbria-Marche earthquake.  
53

### 54 **3.3.1 Margherita Palace and the Civic Tower in L'Aquila** 55

56 The construction of the City Hall in L'Aquila started in 1294 and a first important restoration was  
57 completed in 1541. Important refurbishments were done since 1573, when the building became the house of  
58 Margherita d'Austria, and most of the original characters were lost (Fig. 11a and b). The palace has two floors  
59 and near rectangular plan of about 40 m x 60 m, with an internal court. The vertical structure is made of stone  
60  
61

1 and brick masonry with good mortar. The horizontal structures are made of masonry vaults, partially stabilized  
2 by tyrants. Hidden underground levels could be present under some parts of the building but there is not any  
3 sure information about. The Civic Tower, built from 1254 to 1374 at the N-E corner, was seriously damaged by  
4 the 1703 earthquake and rebuilt with lower height. In 1937 it was consolidated by inserting iron T-beams at the  
5 floors. It has an almost square cross-section of about 6.30 m. The thickness of the walls is equal to 2.0 m at the  
6 basement.

7 The palace suffered heavy damage during the 2009 L'Aquila earthquake. Several cracks were apparent  
8 and local collapse mechanisms were activated. In more details, the seismic event caused the disconnection  
9 between the orthogonal walls, the out-of-plane collapse of some masonry walls, the formation of large cracks,  
10 the collapse of some vaults and important damages to the stairs. For each configuration three tests of about 300 s  
11 were carried out, with a sample rate of 200 point/s using ambient noise as the only source of vibrations. With  
12 this low level of excitation the building showed a quasi-linear behavior, and a spectral analysis could be  
13 performed.

14 Different teams have been monitoring Palazzo Margherita for different goals. In [63] the dynamic  
15 behaviour of the building was analyzed in order to create a reference knowledge in view of an innovative base  
16 isolation design (Fig. 12c). Fifteen seismometers (velocimeter sensors) were deployed in two configurations, the  
17 first one relative to the building and the second to the tower at different levels.

### 20 3.3.2 The Holy Shroud Chapel in Turin

21  
22 Designed by Guarino Guarini to preserve the main relic of Christianity (Fig. 13a-c), built from 1667 to  
23 1694, this outstanding baroque construction was heavily damaged by fire in 1997, right after a general  
24 restoration.

25 After the fire, the Politecnico di Torino was in charge of an experimental campaign on materials and  
26 structure as well as a dynamic test program for the sake of numerical model refinement.

27 On the one hand, in order to collect the data for the design of the structural rehabilitation of the Holy  
28 Shroud Chapel, an extensive campaign of in situ investigations was performed [17]. Visual inspections, laser-  
29 scanning, topographic measures and endoscopy were conducted to achieve a deep knowledge of the structural  
30 morphology of the building (geometry, marble and masonry organization, position of metal ties, etc.). Flat jacks  
31 tests supplied information on the pressures in some critical points; materials mechanical properties were  
32 investigated by laboratory tests on samples, on site sonic tomography and double flat jacks tests. The fire-  
33 induced deterioration of the marble surface was also investigated by means of specific tests.

34 Taking into account these evidences, the structural rehabilitation went through the reconstruction of the  
35 structurally most important parts of the building with new marble elements, produced in the same shape and  
36 extracted from the same mine as the original ones.

37 On the other hand, several vibration tests were executed on the dome, using four different dynamic inputs:

- 38 • Environmental excitation (traffic, wind, micro-quakes);
- 39 • Impulsive excitation produced by hammering;
- 40 • Impulsive excitation caused by dropping a sphere onto the ground near the base of the building;
- 41 • Wind turbulence produced by a Fire-Police helicopter flying around the dome top.

42 A total of 25 accelerometers were used on six different levels, measuring the response in radial, vertical and  
43 tangential directions, and the resulting signals were used to perform the structural identification of the dome. The  
44 output-only modal identification of the structure was obtained through the TFIE method [31] (Fig. 14a).  
45 Impulsive records obtained by dropping the sphere supplied the best results. In this way it was possible to resolve  
46 two modes very close to each other, at  $f_1= 2.246$  Hz and  $f_2= 2.344$  Hz respectively.

47 Results from the experimental dynamic identification were used to perform a stochastic updating of the FE  
48 model of the structure (Fig. 13d). The Probabilistic Global Search Lausanne (PGSL) method was used for the  
49 purpose, belonging to the class of direct, multiple-model updating algorithms [67]. The cost function was set as a  
50 measure of the discrepancy between the identified and the numerical value of the first five modal frequencies and  
51 their corresponding mode-shapes. The updating parameters were chosen to correspond partly to the material  
52 elastic modulus of predefined homogenous substructures of the FE model and partly to the stiffness of spring-type  
53 connections modelling the interaction of the structure with neighboring buildings (Fig. 14b). To reduce the  
54 problem size, data-mining techniques, including  $k$ -means clustering and Principal Components Analysis (PCA),  
55 were used. A preliminary, robust model reconciliation was thus obtained, ultimately resulting in a population of  
56 quasi-optimal models, clustered around five main reference models ("centroids"). As in the case of Vicoforte  
57  
58  
59  
60

1 Sanctuary, the goal was thus achieved of establishing the reference present-state image of the structure in view of  
2 the completion of a FE predictive model which could drive the heavy repair and retrofit made necessary by the  
3 fire damages.  
4

### 5 **3.3.3 CEDRAV building in Cerreto di Spoleto**

6  
7 The building under consideration was built as a monastery in the 14<sup>th</sup> century on the top of the ridge of a  
8 “scaglia rossa” rock formation. Now it is the branch of the Centre for Anthropological Documentation and  
9 Research of the Nera river Valley (CEDRAV). The building is irregular both horizontally and vertically (Fig.  
10 15). The foundations are not at the same level. The first level is partially embedded into the ground and is  
11 mostly founded directly on rock, the second level is partially founded on rock, and the foundation system of the  
12 N-W portion of the building is not known in detail.

13 The building structure is made of stone masonry walls. The first level is divided into three small,  
14 approximately square rooms and a larger rectangular room, from N-E to S-W, used for archiving documents. All  
15 rooms follow an irregular plan. The second level shows, more or less, the same subdivision (there is one small  
16 room missing, the remaining two rooms are merged and the archive is subdivided into two rooms). Then one  
17 more rectangular room in the N-E top and three further ones in the N-W part are present. The room distribution  
18 of the third level is quite similar to that of the second floor, but a small church covered with a cross vault ceiling  
19 is present in the N-E side.

20 Such an articulated construction constitutes the main structure of the CEDRAV building. Three additional  
21 structures are connected to it:

- 22 • a small squared shape structure of three floors at the eastern side;
- 23 • a rectangular building at the northern corner;
- 24 • another rectangular building at the western side, connected to the CEDRAV by means of a masonry  
25 arch.  
26

27 All these connections have a strong influence on the dynamic behaviour of the CEDRAV building. Translational  
28 and torsional frequencies were close to one another, coupling occurred and damping percentage was very low.  
29 As a result, beating effects were quite apparent [68]. The experimental results were compared with those  
30 obtained from FE analysis, which reproduced very well the seismic behaviour except for the beating effects. On  
31 the basis of the experimental results obtained by means of temporary arrays, a permanent network was designed  
32 and installed.  
33

## 34 **3.4 SHM to perform experimental analysis at fixed time intervals and prevent larger damage**

35 SHM can be used to perform long-term, periodical, experimental analysis of damaged historical  
36 constructions at fixed time intervals, in order to control the evolution of their operational response and prevent  
37 development of further damage.  
38

### 39 **3.4.1 The Cochlid Columns in Rome**

40  
41 Among the best-known vestiges of ancient Rome monumental architecture, the Aurelian and Trajan’s  
42 Columns (also called the Cochlid Columns), are both composed by 19 marble blocks carved to obtain a spiral  
43 staircase, the so called cochlea, connecting the central core to the outer ring (Fig. 16). Each block is about 1.5 m  
44 tall, for a total height of the column of about 30 m. The external diameter varies from 3.7 to 3.2 m, while the  
45 diameter of the internal core varies from 1.0 to 0.5 m. Both columns rest on square pedestals. The extent and the  
46 consistency of the underground soil and of the foundations are unknown for both columns [69, 70].

47 In the XVI century, the presence of sliding and rotation among adjacent blocks was noticed in the Aurelian  
48 Column, possibly as a result of earthquakes (Fig. 17). The historical investigations revealed that strong  
49 earthquakes, such of January 22<sup>nd</sup>, 1349, with epicenter in Abruzzo, caused serious damage in Rome and  
50 probably also to the column. This is just an example of the importance of monuments in the study of the  
51 historical seismicity of the Italian territory. The analysis and interpretation of the historical documents should  
52 also account for all the changes occurred in monuments, due to material degradation, changes in loads, seismic  
53 actions, traffic-induced vibrations, presence of other buildings. A suitable study should pass through the  
54 complete historical analysis and the structural health analysis in the present status. This can be done only by  
55 means of a reliable experimental analysis and an accurate numerical modelling, and should also allow the check  
56 of its present structural capacity and the definition of a suitable intervention. It is worth noting that ambient and  
57 traffic-induced vibrations, which contribute to the bad health status of structures, could become very dangerous  
58 when acting on structures already damaged by earthquakes.  
59  
60

1 A first measurement campaign on the Columns was carried out in 1985. Eighteen Teledyne-Geotech  
2 seismometers were used, of which six deployed in the vertical direction and twelve in the horizontal radial and  
3 tangential directions (Fig. 18). Main results can be synthesized as follows:

- 4 • The vibration amplitudes recorded on the Aurelian Column were particularly low, with peak values of  
5 0.32 mm/s along the column, and of 0.15 mm/s on the pedestal; spectral analysis pointed out two  
6 structural resonances at 1.33 and 6.9 Hz;
- 7 • The vibration amplitudes of the Trajan's Column were very low too, with peak values of 0.10 mm/s  
8 along the column, and of 0.05 mm/s on the pedestal; spectral analysis pointed out the first resonance  
9 frequency at 1.60 Hz; other significant peaks were in the range 5.5÷9.0 Hz.

10 FE models of both columns were also set up and manually updating, leading to modal frequencies and  
11 mode-shapes in good agreement with the identified ones. The same models were used to evaluate the seismic  
12 response of the columns according to the response spectrum analysis allowed by the Italian code for low  
13 seismicity areas. The same fundamental frequencies of the two columns were later confirmed by ambient  
14 vibration measurements performed in the '90s.

15 Another experimental campaign was carried out in March 2012. All the recorded data were analyzed in the  
16 frequency domain. The columns showed similar behaviours. The frequencies of the fundamental modes in the  
17 two horizontal directions were 1.24 Hz and 1.30 Hz for the Aurelian Column and 1.45 Hz and 1.51 Hz for the  
18 Trajan's Column. Other amplifications were around 6.50 Hz and in the range between 9.00 and 10.0 Hz for the  
19 Aurelian Column, and between 5.6 and 8.0 Hz and also at 15.6 Hz for the Trajan's Column. Some differences  
20 were also found:

- 21 • in the first two modal shapes of the Aurelian Column the displacements at the base of the pedestal and  
22 at the base of the column are 180° out of phase. This behaviour could be related to a significant rotation  
23 of the pedestal due to soil deformation, and to an ineffective connection between the pedestal and the  
24 column. Furthermore, inelastic rotations could interest the column also along its height; this could  
25 justify the significant amplification at the top;
- 26 • in the vertical direction, a significant amplification is apparent at around 2.00 Hz in the Aurelian  
27 Column, while no significant amplification in the vertical direction appears in the Trajan's Column;
- 28 • The vertical components at the base, mid and top of the columns were examined in the frequency range  
29 1.0÷2.5 Hz. The spectral analysis showed that, at 1.9 Hz, PSDs of recordings in the Aurelian Column  
30 were higher at the top and that the signals were out of phase with a very high value of the coherence  
31 function. These effects can be likely interpreted as due to a rocking motion of the monument. No such  
32 effects were observed in the Trajan's Column.

### 35 36 **3.5 SHM for the early-warning of scouring threats in ancient masonry bridges: a laboratory research** 37 **program at Turin Polytechnic**

38  
39 A special case of SHM is the laboratory research program recently conducted at the Polytechnic of Turin on a  
40 physical scaled model of a two-spans masonry arch bridge. The model was built in order to study the effect of  
41 the central pile settlement due to riverbank erosion and to look for a fast and low-cost early-warning technique  
42 for detecting scouring threats on ancient bridges.

43 The 1:2 scaled model of the masonry arch bridge was built in the laboratory of the Department of  
44 Structural, Building and Geotechnical Engineering at the Politecnico di Torino [71, 72], consisting of a twin-  
45 arch bridge, 5.90 m long, 1.60 m wide and 1.75 m high (Fig. 19). The two arches are segmental arches with a  
46 radius of 2.00 m and an angular opening of 30°. Each span is 2.00 m long between the supports and the  
47 thickness of the arch is equal to 0.20 m. The model was built with handmade clay bricks also scaled to 130 x 65  
48 x 30 mm to respect the adopted modelling scale law. Low compressive strength elements were chosen and a  
49 mortar with poor mechanical properties was used to bind them in order to reproduce the typical materials of  
50 historical constructions. The mid-span masonry pier, which was cut at a hypothetical middle-height section to  
51 allow the insertion of a settlement application system, is imagined to be placed inside the streambed and  
52 subjected to the scour of its foundation. Foundation settlements and rotations were applied on the bridge model  
53 by means of four independent screws installed at the extremities of the settlement application system. The  
54 spherical plain bearings placed at the head of the screws allowed the rotations of the plate which supports the  
55 central pier about the axes parallel to the longitudinal and transversal directions of the bridge.

56 Damage states of increasing extent were introduced to verify the sensitivity of each feature and the  
57 accuracy of the damage detection method. The vibration measurements were acquired after each damage step  
58 using sensors located in different positions on the structure and different sources of excitation.

59 A data-driven approach was chosen as the damage detection method instead of a model-based approach,  
60 whose reliability might be affected by the construction uncertainty and complexity. The damage identification

1 problem is thus treated as a pattern recognition one, where data (patterns) are classified according either to a  
2 priori knowledge or to the statistical information extracted from the patterns. These techniques are particularly  
3 appealing for the assessment of historical structures since their estimation efficacy does not rely on an accurate  
4 physical model but rather on a statistical model established on data-extracted features. The main issue in the  
5 application of data-driven methods concerns the selection of those features which can provide the most  
6 discriminating information about the states of the structure. The sensitivity and the ability to distinguish among  
7 different damage states must be coupled with the requirement of physical meaningfulness to ensure the  
8 reliability and interpretability of the assessment.

9 The Kernel Density Estimation (KDE), in particular, was employed to characterize the correlation between  
10 the vibration signatures acquired in the time domain [73]. The identified natural frequencies and the sampled  
11 range of the transmissibility spectrum were used in the Outlier Analysis (OA) to identify the novelties coming  
12 from the damage steps. All the selected features proved to be sensitive to damage, while showing pros and cons  
13 depending on the feature domain.

14 The diagnostic technique investigated finally proved to be an effective, low cost, non-modal experimental  
15 vibration analysis, capable to detect novelties through outliers of stochastic signal functions, specially promising  
16 for the SHM of historical constructions. Acoustic emission and Brillouin fiber optics in frequency domain have  
17 been later profitably tested on the same object.

## 20 5. Conclusions

21  
22 The structural health monitoring is increasingly emerging as a fundamental tool to ensure a decision-  
23 making support for maintenance and preservation of the architectural heritage worldwide, achieving the  
24 necessary balance between structural safety needs and the respect for its historical and cultural value. From the  
25 achieved experiences we can try to extract some basic conceptual guidelines:

- 26 • a monitoring project shall be often limited and oriented to supply the information mainly required to  
27 build a correct maintenance design and plan;
- 28 • the level of uncertainties in local material properties, local consistency of the masonry texture, non-  
29 documented historical manipulation history is very high in every ancient construction. Building and  
30 updating a predictive numerical model requires assigning averaged geometrical and mechanical  
31 properties, but we shall never forget the spreading of local uncertainties and the consequent risk;
- 32 • the survival of an historical building for a long time, even centuries, does not authorize us to assume  
33 that it won't collapse in the future; degradation, cumulated damages and wrong manipulations can  
34 drastically reduce the safety level;
- 35 • it is not required that all the sensors are absolutely highly sensitive, resolving and accurate; the choice  
36 of resolution and accuracy depends on the specific requested performance. Sometimes a larger number  
37 of cheaper sensors is more useful than a smaller number of expensive-ones, but we need reliable  
38 numerical tools for data interpretation;
- 39 • a predictive numerical model must be "as much simple as possible, as complex as necessary". A wrong  
40 model can't be experimentally amended. A sensitivity based approach can be useful to correctly select  
41 the updatable parameters in a classic update procedure or tentative models in multi-model processes;
- 42 • the model updating process is difficult in massive and irregular masonry constructions due to the global  
43 and local vibration modes closely packed;
- 44 • it is often necessary to keep account of the soil structure interaction to assess a good predictive model.

45  
46  
47 This paper has attempted to throw some light on SHM potential through a brief and inevitably incomplete  
48 review of some of the most significant experiences recently conducted in Italy.

## 50 References

- 51 [1] De Stefano A (2007) Structural identification and health monitoring on the historical architectural heritage.  
52 Key Eng Mat 347:37-54
- 53 [2] Italian Presidency of the Council of Ministers (2008) Direttiva del presidente del Consiglio dei Ministri per  
54 la valutazione e la riduzione del rischio sismico del patrimonio culturale con riferimento alle norme  
55 tecniche per le costruzioni, Suppl. Ord. alla Gazzetta ufficiale, n. 24, 29 gennaio 2008 [in Italian]. Rome,  
56 Italy: Istituto Poligrafico della Zecca di Stato
- 57 [3] Binda L, Saisi A, Tiraboschi C (2000) Investigation procedures for the diagnosis of historic masonries.  
58 Constr Build Mater 14:199-233

- 1 [4] De Stefano A, Ceravolo R (2007) Assessing the health state of ancient structures: the role of vibrational  
2 tests. *J Intel Mat Syst Str* 18:793-807
- 3 [5] Cabboi A, Gentile C, Guidobaldi M, Saisi A (2015) Continuous dynamic monitoring of historic masonry  
4 towers using few accelerometers: methodological aspects and typical results. In: Proc. 7<sup>th</sup> Int. Conf. on  
5 Structural Health Monitoring of Intelligent Infrastructures, Turin, Italy, July 1-3 2015
- 6 [6] Galleani L, Lo Presti L, De Stefano A (1998) A method for nonlinear system classification in the time  
7 Frequency plane. *Signal Process* 65:147-153
- 8 [7] Vestroni F, Beolchini GC, Antonacci E, Modena C (1991) Identification of dynamic characteristics of  
9 masonry buildings from forced vibration tests. In: Proc. 11th World Conf. on Earthquake Eng., Elsevier,  
10 paper 1165, ISBN 0080428223
- 11 [8] Cempel C (2003) Multidimensional condition monitoring of mechanical systems in operation. *Mech Syst*  
12 *Signal Pr* 17(3):1291-1303
- 13 [9] De Stefano A, Matta E (2008) Risk, reliability, uncertainties: role and strategies for the structural health  
14 monitoring. In: Pasman H and Kirillov IA (ed) Resilience of cities to terrorist and other threats: learning  
15 from 9/11 and further research issues. Springer, Amsterdam, pp 301-324
- 16 [10] Lawless JF (1982) Statistical models and methods for lifetime data. J. Wiley & Sons, NY
- 17 [11] Natke HG, Cempel C (2001) System observation matrix for monitoring and diagnosis. *J. Sound Vib*  
18 248:597-620
- 19 [12] Cempel C, Tabszewski M (2007) Multidimensional condition monitoring of machines in non-stationary  
20 operation. *Mech Syst Signal Pr* 21:1233-1241
- 21 [13] De Stefano A (2014) On-line monitoring and resilient design for a longer construction life. In: Proc. of the  
22 46th ESReDA Seminar, Turin, Italy, May 29-30 2014
- 23 [14] De Stefano A, Clemente P (2005) S.H.M. on historical heritage: robust methods to face large uncertainties.  
24 In: Proc. 1<sup>st</sup> Int. Conf. on Structural Condition Assessment, Monitoring and Improvement (key-note  
25 lecture), Perth, W.A.
- 26 [15] Smith IFC, Saitta S, Ravindran S, Kripakaran P (2006) Challenges of data interpretation. In: Proc. 18<sup>th</sup>  
27 SAMCO Workshop, pp 37-57.
- 28 [16] Matta E., De Stefano A (2012) Robust finite element model updating of a large-scale benchmark building  
29 structure. *Struct Eng Mech* 43:371-394
- 30 [17] De Stefano A (2009) SHM actions on the Holy Shroud Chapel in Torino. In: Boller C., Chang F-K, Fujino  
31 Y (ed) Encyclopedia of Structural Health Monitoring. Wiley&sons, Chichester, Vol. 4 Chapter 132. ISBN:  
32 9780470058220
- 33 [18] Chiarugi A, Bartoli G, Morano SG (1998) The surveillance of Brunelleschi dome in Florence. In: Proc. 2nd  
34 Int. Conf. on Structural Analysis of Historic Construction, pp 337-354.
- 35 [19] Gabbanini F, Vannucci M (2004) Wavelet packet methods for the analysis of variance of time series with  
36 Application to crack widths on the Brunelleschi Dome. *J Comput Graph Stat* 13(3):639-658
- 37 [20] Blasi C, Ottoni F (2012) New studies on Brunelleschi's Dome in Florence from historical to modern  
38 monitoring data analysis. The effect of encircling scaffoldings on cracks evolution. In: Proc. of Domes in  
39 the World, Florence, 19-23 March 2012
- 40 [21] Bongiovanni G, Celebi M, Clemente P (1990) The Flaminio Obelisk in Rome: vibrational characteristics as  
41 part of preservation efforts. *Earthquake Eng Struc*, John Wiley & Sons, Vol. 19, 107-118, ISSN 0098-  
42 8847.90.010107
- 43 [22] Lorenzoni F, Casarin F, Modena C, Caldon M, Islami K, Da Porto F (2013) Structural health monitoring of  
44 the Roman Arena of Verona. *J Civil Structural Health Monitoring* 3:227-246, ISSN 2190-5452, DOI  
45 10.1007/S13349-013-0065-0
- 46 [23] Ceriotti M, Mottola L, Picco GP, Murphy AL, Gună Ş, Corrà M, Pozzi M, Zonta D, Zanon P (2009)  
47 Monitoring heritage building with wireless sensor networks: the Torre Aquila deployment. In: Proc. 8th Int.  
48 Conf. on Information Processing in Sensor Networks
- 49 [24] Zonta D, Pozzi M, Zanon P, Anese GA, Busetto A (2008) Real-time probabilistic health monitoring of the  
50 Portogruaro Civic Tower. In: D'Ayala D, Fodde E (ed) Structural Analysis of Historic Construction, Taylor  
51 & Francis, London, pp 723-731. ISBN: 0415468728
- 52 [25] Rossi PP, Rossi C (2015) Monitoring of two great Venetian Cathedrals: San Marco and Santa Maria  
53 Gloriosa dei Frari. *Int J of Archit Herit* 9:58-81
- 54 [26] Pau A, Vestroni F (2013) Vibration assessment and structural monitoring of the Basilica of Maxentius in  
55 Rome. *Mech Syst Signal Pr* 41(1-2):454-466
- 56 [27] Gattulli V, Graziosi F, Federici F, Potenza F, Colarieti A, Lepidi M (2013) Structural health monitoring of  
57 the Basilica S. Maria di Collemaggio. In: Proc. 5<sup>th</sup> Int. Conf. on Structural Engineering, Mechanics and  
58 Computation, Cape Town, 2-4 Sept 2013, pp 823-824
- 59  
60  
61  
62  
63  
64  
65

- 1 [28] Zonta D, Ceravolo R, Bursi O, Erlicher S, Zanon P, De Stefano A (2002) Issues on vibration-based  
2 identification of complex monumental structures: the Dome of S. Gaudenzio Church in Novara. In: Proc. 3<sup>rd</sup>  
3 World Conf. on Structural Control, Como, Italy
- 4 [29] Brincker R, Zhang L, Andersen P (2001) Modal identification of output-only systems using frequency  
5 domain decomposition. *Smart Mater Struct* 10(3):441-445
- 6 [30] Juang JN, Pappa RS (1984) An eigensystem realisation algorithm (ERA) for modal parameter identification  
7 and modal reduction. Proc. NASA/JPL Workshop on Identification and Control of Flexible Space  
8 Structures
- 9 [31] Bonato P, Ceravolo R, De Stefano A, Molinari F (2001) Use of cross time–frequency estimators for the  
10 structural identification in non-stationary conditions and under unknown excitation. *J Sound Vib* 237:775-  
11 791
- 12 [32] De Stefano A, Matta E, Quattrone A (2009) Improvement of Time-Frequency domain identification  
13 through PCA. In: Proc. 3<sup>th</sup> Int. Conf. on Operational Modal Analysis, Portonovo, Italy, May 4-6, 2009
- 14 [33] Zanon P, Bursi OS, Erlicher S, Zonta D, Clemente P, Indirli M (2001) Intervention scenarios on the  
15 Basilica of San Gaudenzio dome in Novara. In: Proc. 7<sup>th</sup> Int. Seminar on Seismic Isolation, Passive Energy  
16 Dissipation and Active Control of Vibrations of Structures, GLIS and EAEE-TG5, Vol. 2(34), Assisi, Italy,  
17 Oct. 2-5 2001, pp 285-292
- 18 [34] Chiorino MA, Spadafora A, Calderini C, Lagomarsino S (2008) Modeling strategies for the world largest  
19 elliptical dome at Vicoforte. *Int J Arch Herit* 2:274-303
- 20 [35] Chiorino MA, Ceravolo R, Spadafora A, Zanutti Fragonara L, Abbiati G (2011) Dynamic characterization  
21 of complex masonry structures: the Sanctuary of Vicoforte. *Int J Arch Herit* 5(3): 296-314
- 22 [36] Ceravolo R, Chiorino MA, Lai C, Pecorelli ML, Zanutti Fragonara L, Analysis of long-term monitoring  
23 data to assess the efficacy of tie-bars strengthening interventions on a large historical dome. In: Proc. 7<sup>th</sup> Int.  
24 Conf. on Structural Health Monitoring of Intelligent Infrastructures, Turin, Italy, July 1-3 2015
- 25 [37] Allemang RJ (2002) The Modal Assurance Criterion (MAC): twenty years of use and abuse. In: Proc. 20<sup>th</sup>  
26 Int. Modal Analysis Conference, Los Angeles, CA, February 4-7 2002, pp 397-405
- 27 [38] Van Overschee P, De Moor B (1996) Subspace identification for linear systems: theory-implementation-  
28 applications, Kluwer Academic Publishers, Dordrecht, the Netherlands
- 29 [39] Sabia D, Aoki T, Cosentini RM, Lancellotta R (2015) Model updating to forecast the dynamic behaviour of  
30 the Ghirlandina Tower in Modena, Italy. *J Earthq Eng* 19(1):1-24. DOI: 10.1080/13632469.2014.962668
- 31 [40] Pisanò F, Di Prisco CG, Lancellotta R (2014) Soil-foundation modelling in laterally loaded historical  
32 towers. *Géotechnique* 64(1):1-15
- 33 [41] Lancellotta R, Sabia D (2013) The role of monitoring and identification techniques on the preservation of  
34 historic towers. In: Proc. 2<sup>nd</sup> Int. Symposium on Geotechnical Eng. for the Preservation of Monuments and  
35 Historic Sites (special lecture), Naples, Italy, CRC Press, Taylor and Francis
- 36 [42] Friswell MI, Mottershead JE (1995) Finite element model updating in structural dynamics, Kluwer  
37 Academic Publishers, Dordrecht, the Netherlands
- 38 [43] Reynolds P, Pavic A (2000) Quality assurance procedures for the modal testing of building floor structures.  
39 *ExpTechniques* 24(4):36-41
- 40 [44] Lancellotta R, Sabia D (2013) Identification technique for soil-structure analysis of the Ghirlandina  
41 tower. *Int J Arch Herit* (in press). DOI:10.1080/15583058.2013.793438
- 42 [45] Wu JR, Li QS (2004) Finite element model updating for a high-rise structure based on ambient vibration  
43 measurements. *Eng Struct* 26:979-990
- 44 [46] Mottershead JE, Link M, Friswell MI (2011) The sensitivity method in finite element model updating: a  
45 tutorial. *Mech Syst Signal Pr* 25:2275-2296
- 46 [47] Clemente P, Buffarini G (1998) Seismic performance of the Duomo of Orvieto. In: Proc. Monument-98 -  
47 Workshop on Seismic Performance of Monuments, Lisboa, 12-14 Nov, pp 47-56
- 48 [48] Buffarini G, Clemente P, Paciello A, Rinaldis D (2008) Vibration analysis of the Lateran Obelisk. In: Proc.  
49 14th World Conf. on Earth. Eng., Beijing, 12-17 Oct, IAEE & CAEE, Mira Digital Publishing, Saint Louis,  
50 paper S11-055
- 51 [49] Buffarini G, Clemente P, Paciello A, Rinaldis D (2009) The Lateran Obelisk: experimental analysis and  
52 modelling. In: Proc. Int. Conf. on Protection of Historical Buildings, Rome, Italy, 21-24 June 2009, Vol. 1,  
53 pp 841-848, Taylor & Francis Group, London, ISBN 978-0-415-55803-7
- 54 [50] Lorenzoni F (2013) Integrated methodologies based on structural health monitoring of cultural heritage  
55 buildings, PhD Thesis, Trento
- 56 [51] Modena C (2015) Structural Health Monitoring: a tool for managing risks in sub-standard conditions. In:  
57 Proc. 7<sup>th</sup> Int. Conf. on Structural Health Monitoring of Intelligent Infrastructures (key-note lecture), Turin,  
58 Italy, July 1-3 2015

- 1 [52] Burland JB, Jamiolkowski MB, Viggiani C (2009) Leaning Tower of Pisa: behaviour after stabilization  
2 operations. *Int J Geoenviron Eng* 1(3):156-169
- 3 [53] Del Grosso A, Torre A, Rosa M, Lattuada B (2004) Application of SHM techniques in the restoration of  
4 historical buildings: the Royal Villa of Monza. In: *Proc. 2<sup>nd</sup> European Conf. on Health Monitoring*, Munich,  
5 Germany, July 7-9 2004
- 6 [54] Bongiovanni G, Buffarini G, Clemente P, Rinaldis D, Saitta F, Nicoletti M, De Sortis A, Rossi G (2013).  
7 Dynamic identification of Palazzo Marchesale in S. Giuliano di Puglia. In: *Proc. 5<sup>th</sup> Int. Conf. on Structural*  
8 *Engineering, Mechanics and Computation*, Cape Town, 2-4 Sept 2013, pp 81–86. ISBN 978-1-136-00061-  
9 2
- 10 [55] Buffarini G., Clemente P., Rinaldis D. 1997, Tempio Rotondo al Foro Boario: Rilievo delle vibrazioni  
11 ambientali (1a fase: Struttura non consolidata), RT/AMB/97/11, ENEA, Roma, and Buffarini G., Clemente  
12 P., Rinaldis D. 1997. Tempio Rotondo al Foro Boario: Rilievo delle vibrazioni ambientali. 2a Fase.  
13 RT/AMB/97/12, ENEA, Roma
- 14 [56] Buffarini G, Clemente P, Rinaldis D (1997) Tempio Rotondo al Foro Boario: rilievo delle vibrazioni  
15 ambientali - 1a Fase: struttura non consolidata. RT/AMB/97/11, ENEA, Roma
- 16 [57] Buffarini G, Clemente P, Rinaldis D (1997) Tempio Rotondo al Foro Boario: rilievo delle vibrazioni  
17 ambientali - 2a Fase. RT/AMB/97/12, ENEA, Roma
- 18 [58] Bongiovanni G., Clemente P., Buffarini G. (2000) Analysis of the seismic response of a damaged masonry  
19 bell tower. *Proc.*, 12 World Conf. on Earth. Eng. (Auckland, 30 Jan – 4 Feb), Paper 2189.
- 20 [59] Clemente P, Bongiovanni G, Buffarini G (2002) Experimental analysis of the seismic behaviour of a  
21 cracked masonry structure. In: *Proc. 12<sup>th</sup> European Conf. on Earthquake Eng.*, Elsevier Science Ltd,  
22 London 9-13 Sept 2002, paper 104
- 23 [60] Indirli M, Castellano MG, Clemente P, Martelli A (2001) Demo application of shape memory alloy devices:  
24 the rehabilitation of S. Giorgio Church in Trignano. In: *Proc. SPIE's 8th Annual Int. Symposium on Smart*  
25 *Structures and Materials*, Newport Beach, 4-8 Mar 2001
- 26 [61] Clemente P., Rinaldis D., Bongiovanni G. (1994). "Dynamic characteristics of a non-seismic masonry  
27 building". In Davidovici V. & Benedetti D. (ed) *Strengthening and Repair of Structures in Seismic Area*,  
28 OUEST ÉDITIONS (for AFPS-ANIDIS), Nantes, 243-252, ISBN 2-908261-04-9.
- 29 [62] Buffarini G, Clemente P, Rinaldis D (1996) Vibration test of an old masonry building. In: *Proc.*  
30 *Eurodyn'96*, Balkema, Rotterdam, Vol. 2, pp 825-832. ISBN 90-5410-813-4
- 31 [63] Buffarini G, Cimellaro G, Clemente P, De Stefano A (2011) Experimental dynamic analysis of Palazzo  
32 Margherita after the April 6<sup>th</sup>, 2009, earthquake. In: *Proc. 4<sup>th</sup> Int. Conf. on Experimental Analysis for Civil*  
33 *Engineering Structures (EVACES 2011)*, Varenna, Italy, 3-5 Oct 2011, pp 247-254. ISBN 978-88-96225-  
34 39-4
- 35 [64] De Stefano A, Enrione D, Ruocci G (2008) Innovative techniques for structural assessment: the case of the  
36 Holy Shroud Chapel in Turin. In: *Proc. 6<sup>th</sup> Int. Conf. on Structural Analysis of Historic Construction*, Vol.  
37 1, Bath, Great Britain, July 2-4 2008, pp 575-582. ISBN: 9780415468725
- 38 [65] De Stefano A, Clemente P (2009) Structural health monitoring of historic buildings". In: Karbhari VM,  
39 Ansari F (eds) *Structural Health Monitoring of Civil Infrastructure Systems*, Woodhead Publishing Ltd.  
40 ISBN 9781845693923
- 41 [66] Russo S (2013) On the monitoring of historic Anime Sante church damaged by earthquake in L'Aquila.  
42 *Struct Control Hlth* 20(9):1226-1239
- 43 [67] Smith IFC (2005) Multi-model interpretation of measurement data with errors, *CANSMART 2005*, RMC,  
44 Canada, pp 13-22
- 45 [68] Clemente P., Rinaldis D., Buffarini G. (2007) Experimental seismic analysis of a historical building.  
46 *Journal of Intelligent Material Systems and Structures*, Vol. 18, No. 8, 777-784.
- 47 [69] Bongiovanni G, Buffarini G, Clemente P, Saitta F (2014) Dynamic characterization of the Trajan's Column.  
48 In: *Proc. 9<sup>th</sup> Int. Conf. on Structural Analysis of Historical Constructions, SAHC2014*, Mexico City, 15-17  
49 Oct. ISBN 04-2014-102011495500-102
- 50 [70] Bongiovanni G, Buffarini G, Clemente P, Saitta F (2014) Ambient vibrational analysis of Aurelian Column.  
51 In: *Proc. 10<sup>th</sup> U.S. National Conf. on Earth. Eng. (10NCEE)*, Earth. Eng. Research Institute, Anchorage,  
52 AK, 21-25 July, paper 1013
- 53 [71] Ruocci G, Quattrone A, De Stefano A (2011) Multi-domain feature selection aimed at the damage detection  
54 of historical bridges. *Journal of Physics, Conference Series* 305, pp 1-10. ISSN: 1742-6588
- 55 [72] Zanotti Fragonara L, Ceravolo R, Matta E, Quattrone A, De Stefano A, Pecorelli M (2012) Non-linear  
56 characterisation of the physical model of an ancient masonry bridge. *Journal of Physics, Conference Series*  
57 382. ISSN: 1742-6588
- 58 [73] Parzen E (1962) On estimation of a probability density function and mode. *Ann Math Stat* 33:1065-1076

1  
2  
3  
4  
5  
6  
7  
8  
9  
10  
11  
12  
13  
14  
15  
16  
17  
18  
19  
20  
21  
22  
23  
24  
25  
26  
27  
28  
29  
30  
31  
32  
33  
34  
35  
36  
37  
38  
39  
40  
41  
42  
43  
44  
45  
46  
47  
48  
49  
50  
51  
52  
53  
54  
55  
56  
57  
58  
59  
60  
61  
62  
63  
64  
65

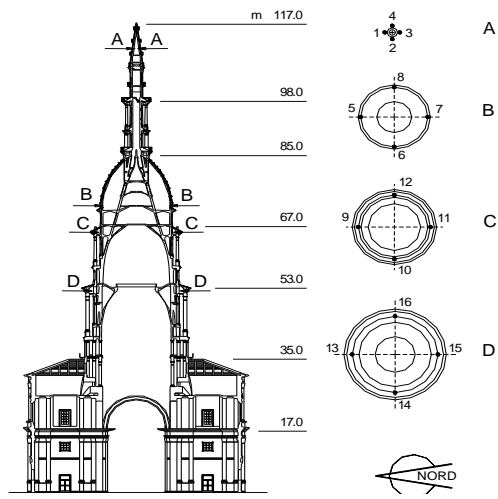


**Fig. 1** The Roman Arena in Verona

1  
2  
3  
4  
5  
6  
7  
8  
9  
10  
11  
12  
13  
14  
15  
16  
17  
18  
19  
20  
21  
22  
23  
24  
25  
26  
27  
28  
29  
30  
31  
32  
33  
34  
35  
36  
37  
38  
39  
40  
41  
42  
43  
44  
45  
46  
47  
48  
49  
50  
51  
52  
53  
54  
55  
56  
57  
58  
59  
60  
61  
62  
63  
64  
65



(a)



(b)

**Fig. 2** The dome of S. Gaudenzio Church in Novara: (a) overall view; (b) vertical section

1  
2  
3  
4  
5  
6  
7  
8  
9  
10  
11  
12  
13  
14  
15  
16  
17  
18  
19  
20  
21  
22  
23  
24  
25  
26  
27  
28  
29  
30  
31  
32  
33  
34  
35  
36  
37  
38  
39  
40  
41  
42  
43  
44  
45  
46  
47  
48  
49  
50  
51  
52  
53  
54  
55  
56  
57  
58  
59  
60  
61  
62  
63  
64  
65

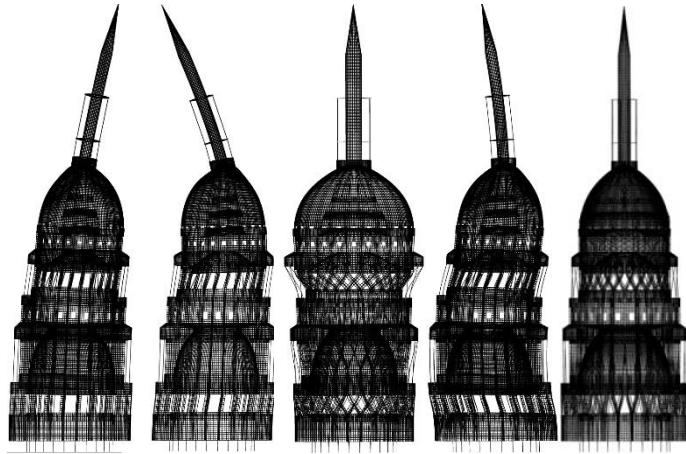


**Fig. 3.** Graphical representation of the first 5 mode shapes obtained through the updated FE model.

1  
2  
3  
4  
5  
6  
7  
8  
9  
10  
11  
12  
13  
14  
15  
16  
17  
18  
19  
20  
21  
22  
23  
24  
25  
26  
27  
28  
29  
30  
31  
32  
33  
34  
35  
36  
37  
38  
39  
40  
41  
42  
43  
44  
45  
46  
47  
48  
49  
50  
51  
52  
53  
54  
55  
56  
57  
58  
59  
60  
61  
62  
63  
64  
65



**Fig. 4** The Sanctuary of Vicoforte: (a) exterior view; (b) interior view of the elliptic dome

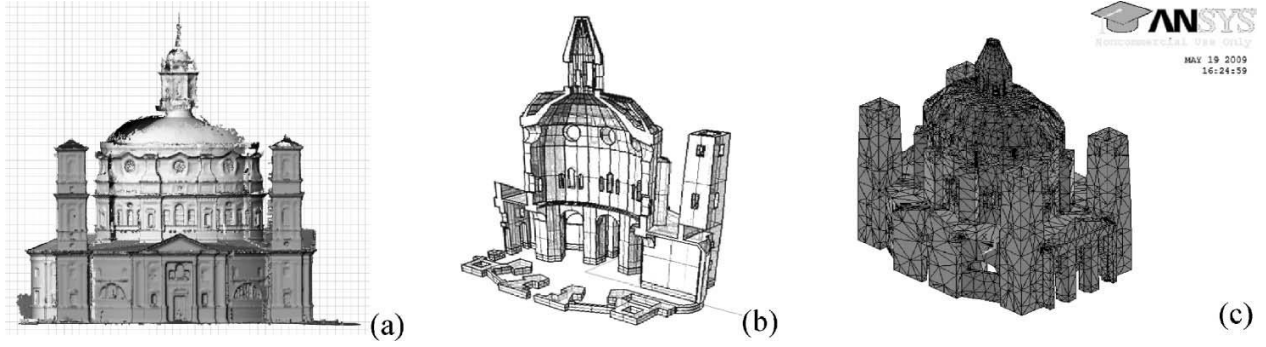


**Fig. 5** The Sanctuary of Vicoforte: (a) cluster of points obtained with a laser scanner; (b) axonometric split view of the geometric model; (c) finite model element (FEM)

1  
2  
3  
4  
5  
6  
7  
8  
9  
10  
11  
12  
13  
14  
15  
16  
17  
18  
19  
20  
21  
22  
23  
24  
25  
26  
27  
28  
29  
30  
31  
32  
33  
34  
35  
36  
37  
38  
39  
40  
41  
42  
43  
44  
45  
46  
47  
48  
49  
50  
51  
52  
53  
54  
55  
56  
57  
58  
59  
60  
61  
62  
63  
64  
65

1  
2  
3  
4  
5  
6  
7  
8  
9  
10  
11  
12  
13  
14  
15  
16  
17  
18  
19  
20  
21  
22  
23  
24  
25  
26  
27  
28  
29  
30  
31  
32  
33  
34  
35  
36  
37  
38  
39  
40  
41  
42  
43  
44  
45  
46  
47  
48  
49  
50  
51  
52  
53  
54  
55  
56  
57  
58  
59  
60  
61  
62  
63  
64  
65



**Fig. 6** The Ghirlandina Tower in Modena

1  
2  
3  
4  
5  
6  
7  
8  
9  
10  
11  
12  
13  
14  
15  
16  
17  
18  
19  
20  
21  
22  
23  
24  
25  
26  
27  
28  
29  
30  
31  
32  
33  
34  
35  
36  
37  
38  
39  
40  
41  
42  
43  
44  
45  
46  
47  
48  
49  
50  
51  
52  
53  
54  
55  
56  
57  
58  
59  
60  
61  
62  
63  
64  
65

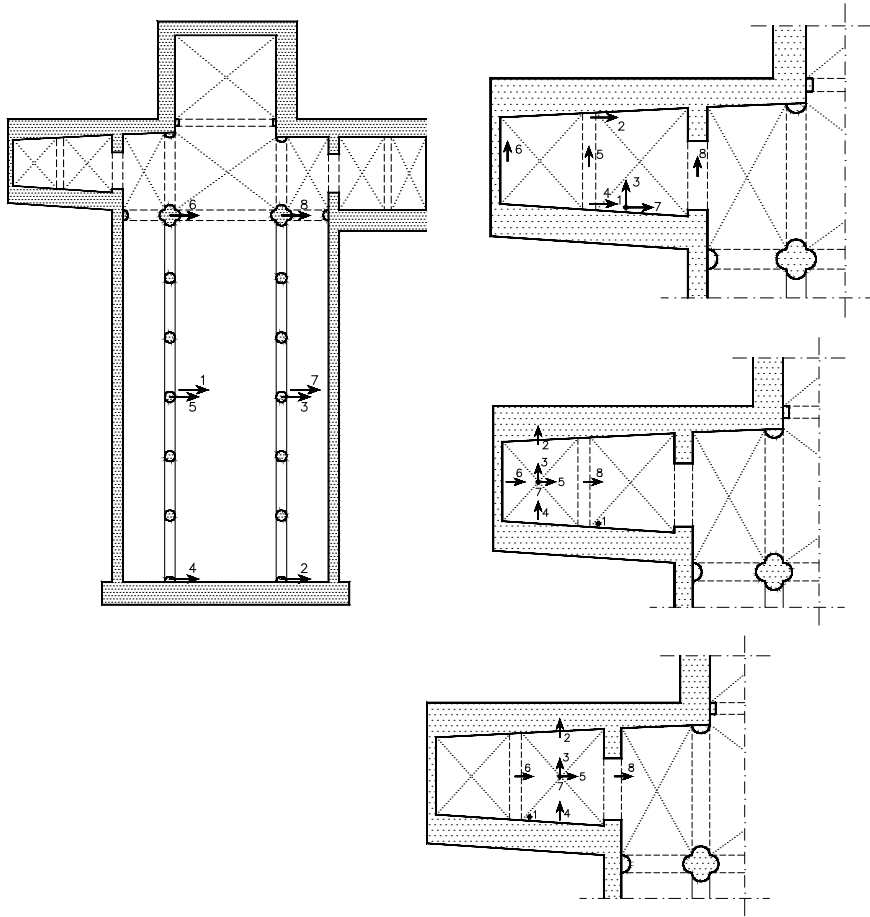


**Fig. 7** Sensor deployment in the Duomo of Orvieto

1  
2  
3  
4  
5  
6  
7  
8  
9  
10  
11  
12  
13  
14  
15  
16  
17  
18  
19  
20  
21  
22  
23  
24  
25  
26  
27  
28  
29  
30  
31  
32  
33  
34  
35  
36  
37  
38  
39  
40  
41  
42  
43  
44  
45  
46  
47  
48  
49  
50  
51  
52  
53  
54  
55  
56  
57  
58  
59  
60  
61  
62  
63  
64  
65

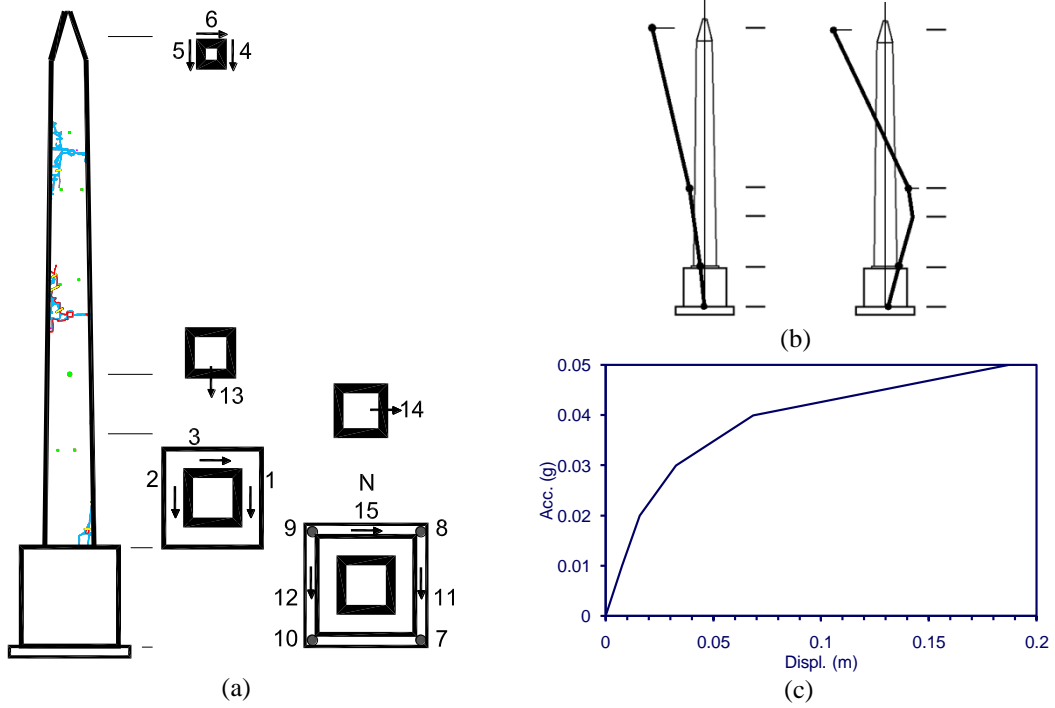


**Fig. 8** The Lateran Obelisk in Rome: (a) seismometer locations; (b) N-S modal shapes; (c) acceleration-displacement diagram

1  
2  
3  
4  
5  
6  
7  
8  
9  
10  
11  
12  
13  
14  
15  
16  
17  
18  
19  
20  
21  
22  
23  
24  
25  
26  
27  
28  
29  
30  
31  
32  
33  
34  
35  
36  
37  
38  
39  
40  
41  
42  
43  
44  
45  
46  
47  
48  
49  
50  
51  
52  
53  
54  
55  
56  
57  
58  
59  
60  
61  
62  
63  
64  
65

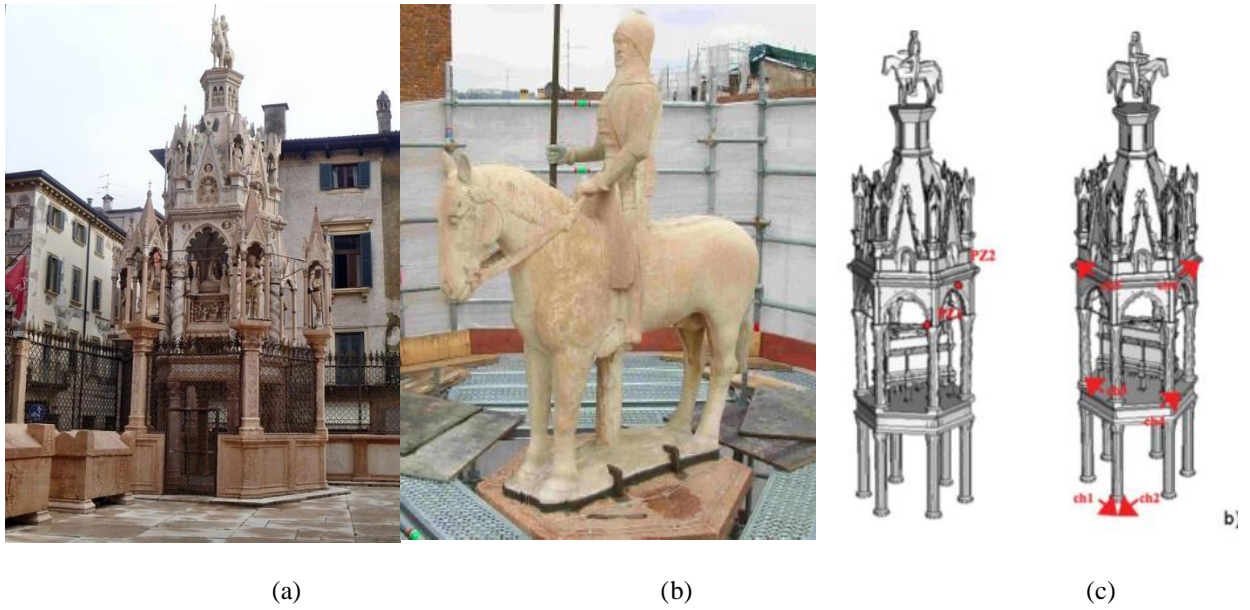


**Fig. 9** Cansignorio stone tomb: (a) overall view; (b) the equestrian statue; (c) sensors layout (left: static transducers on cracks; right: mono-axial accelerometers)

1  
2  
3  
4  
5  
6  
7  
8  
9  
10  
11  
12  
13  
14  
15  
16  
17  
18  
19  
20  
21  
22  
23  
24  
25  
26  
27  
28  
29  
30  
31  
32  
33  
34  
35  
36  
37  
38  
39  
40  
41  
42  
43  
44  
45  
46  
47  
48  
49  
50  
51  
52  
53  
54  
55  
56  
57  
58  
59  
60  
61  
62  
63  
64  
65

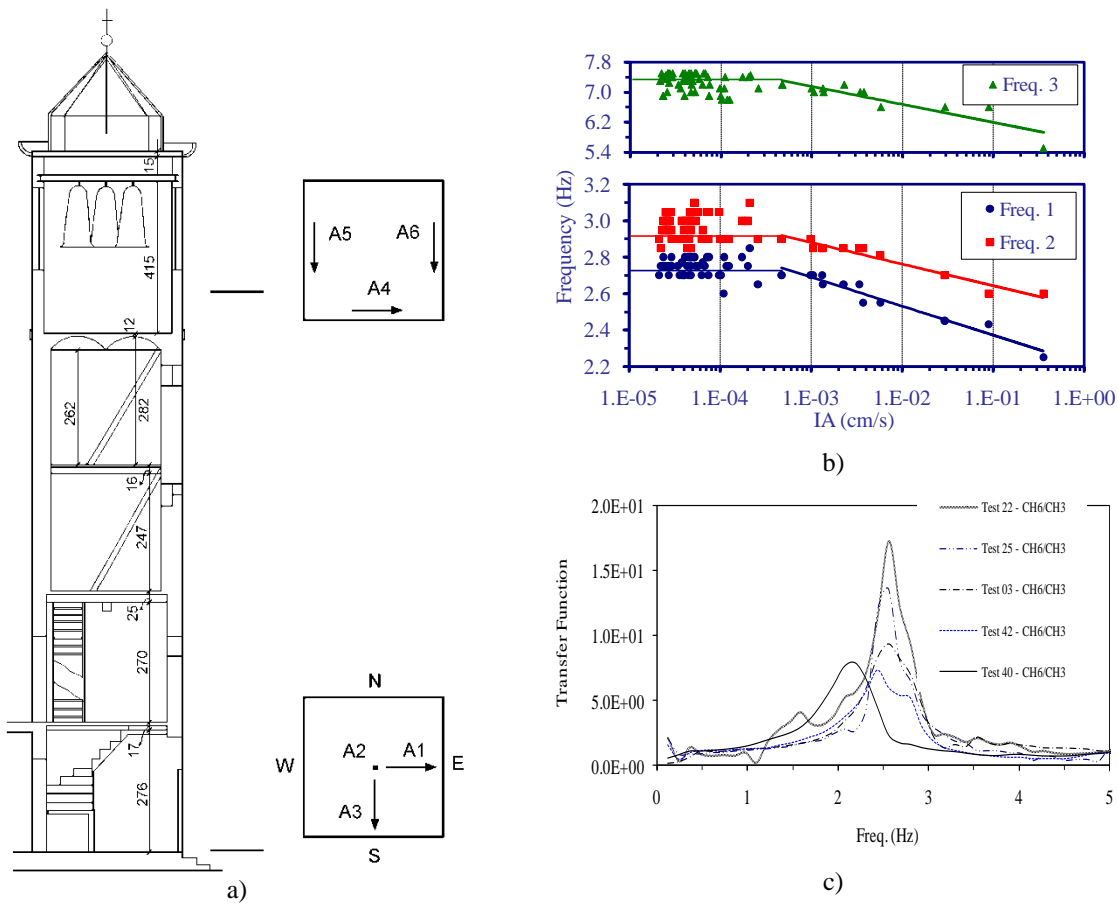


**Fig. 10** The Bell Tower of S. Giorgio in Trignano: (a) accelerometers layout; (b) frequencies versus IA; (c) transfer functions for events having increasing intensity

1  
2  
3  
4  
5  
6  
7  
8  
9  
10  
11  
12  
13  
14  
15  
16  
17  
18  
19  
20  
21  
22  
23  
24  
25  
26  
27  
28  
29  
30  
31  
32  
33  
34  
35  
36  
37  
38  
39  
40  
41  
42  
43  
44  
45  
46  
47  
48  
49  
50  
51  
52  
53  
54  
55  
56  
57  
58  
59  
60  
61  
62  
63  
64  
65

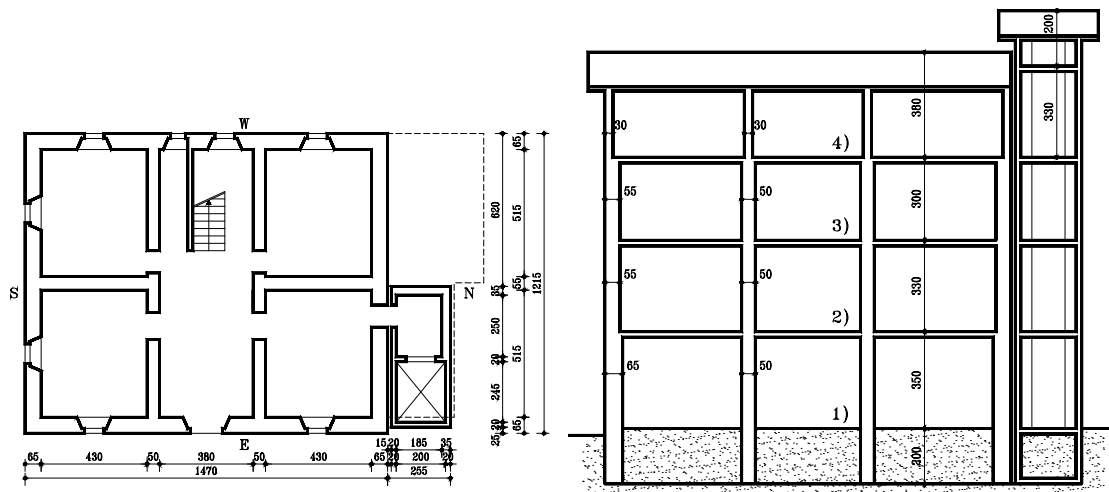
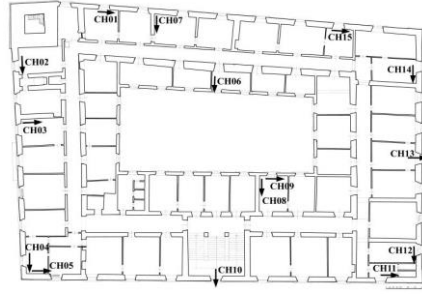


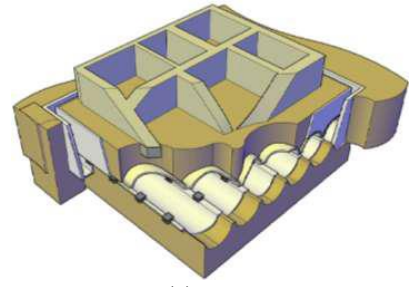
**Fig. 11** The Hospital in Pievepelago: plan and vertical section of the building



(a)



(b)



(c)

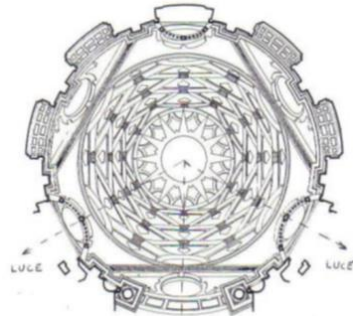
**Fig. 12** Palazzo Margherita and Civic Tower: (a) front; (b) plan; (c) underground isolation (Patent PCT d.n. PCT/IB2011/000716, april 02, 2011 Politecnico di Torino-ENEA)



(a)



(b)



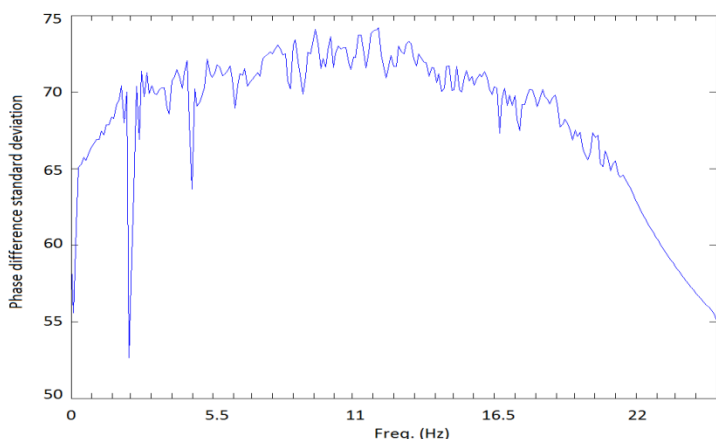
(c)



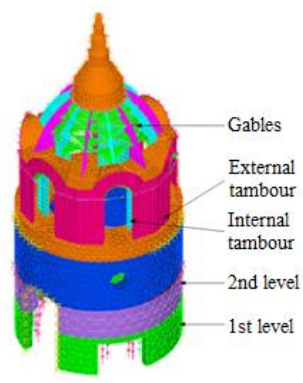
(d)

**Fig. 13** The Holy Shroud Chapel: (a) photo; (b) and (c) draws; (d) FEM view

1  
2  
3  
4  
5  
6  
7  
8  
9  
10  
11  
12  
13  
14  
15  
16  
17  
18  
19  
20  
21  
22  
23  
24  
25  
26  
27  
28  
29  
30  
31  
32  
33  
34  
35  
36  
37  
38  
39  
40  
41  
42  
43  
44  
45  
46  
47  
48  
49  
50  
51  
52  
53  
54  
55  
56  
57  
58  
59  
60  
61  
62  
63  
64  
65



(a)



(b)

**Fig. 14** The Holy Shroud Chapel: (a) TFIE (frequencies as downward peaks); (b) Model homogenous segments

1  
2  
3  
4  
5  
6  
7  
8  
9  
10  
11  
12  
13  
14  
15  
16  
17  
18  
19  
20  
21  
22  
23  
24  
25  
26  
27  
28  
29  
30  
31  
32  
33  
34  
35  
36  
37  
38  
39  
40  
41  
42  
43  
44  
45  
46  
47  
48  
49  
50  
51  
52  
53  
54  
55  
56  
57  
58  
59  
60  
61  
62  
63  
64  
65

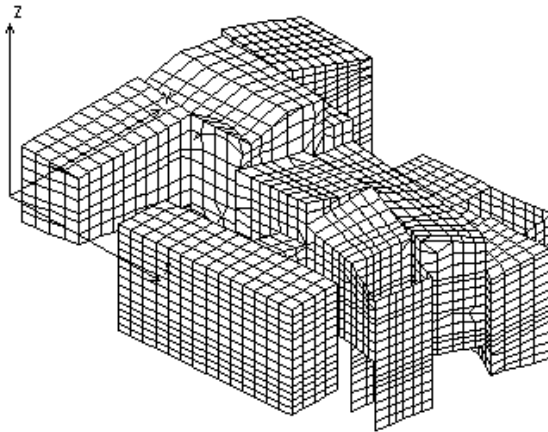


**Fig. 15** The CEDRAV building: axonometric view of the FE model

1  
2  
3  
4  
5  
6  
7  
8  
9  
10  
11  
12  
13  
14  
15  
16  
17  
18  
19  
20  
21  
22  
23  
24  
25  
26  
27  
28  
29  
30  
31  
32  
33  
34  
35  
36  
37  
38  
39  
40  
41  
42  
43  
44  
45  
46  
47  
48  
49  
50  
51  
52  
53  
54  
55  
56  
57  
58  
59  
60  
61  
62  
63  
64  
65



(a)



(b)

**Fig. 16** (a) The Aurelian Column and (b) the Trajan's Column

1  
2  
3  
4  
5  
6  
7  
8  
9  
10  
11  
12  
13  
14  
15  
16  
17  
18  
19  
20  
21  
22  
23  
24  
25  
26  
27  
28  
29  
30  
31  
32  
33  
34  
35  
36  
37  
38  
39  
40  
41  
42  
43  
44  
45  
46  
47  
48  
49  
50  
51  
52  
53  
54  
55  
56  
57  
58  
59  
60  
61  
62  
63  
64  
65



**Fig. 17** The Aurelian Column: relative dislocation between two adjacent blocks

1  
2  
3  
4  
5  
6  
7  
8  
9  
10  
11  
12  
13  
14  
15  
16  
17  
18  
19  
20  
21  
22  
23  
24  
25  
26  
27  
28  
29  
30  
31  
32  
33  
34  
35  
36  
37  
38  
39  
40  
41  
42  
43  
44  
45  
46  
47  
48  
49  
50  
51  
52  
53  
54  
55  
56  
57  
58  
59  
60  
61  
62  
63  
64  
65

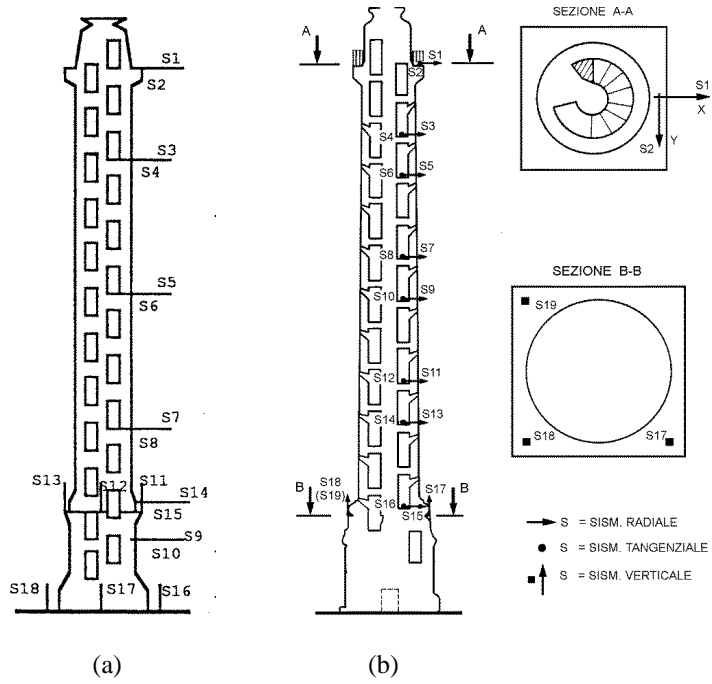


**Fig. 18** Sensors deployment in the 1985 campaign: (a) the Aurelian and (b) the Trajan's Columns

1  
2  
3  
4  
5  
6  
7  
8  
9  
10  
11  
12  
13  
14  
15  
16  
17  
18  
19  
20  
21  
22  
23  
24  
25  
26  
27  
28  
29  
30  
31  
32  
33  
34  
35  
36  
37  
38  
39  
40  
41  
42  
43  
44  
45  
46  
47  
48  
49  
50  
51  
52  
53  
54  
55  
56  
57  
58  
59  
60  
61  
62  
63  
64  
65

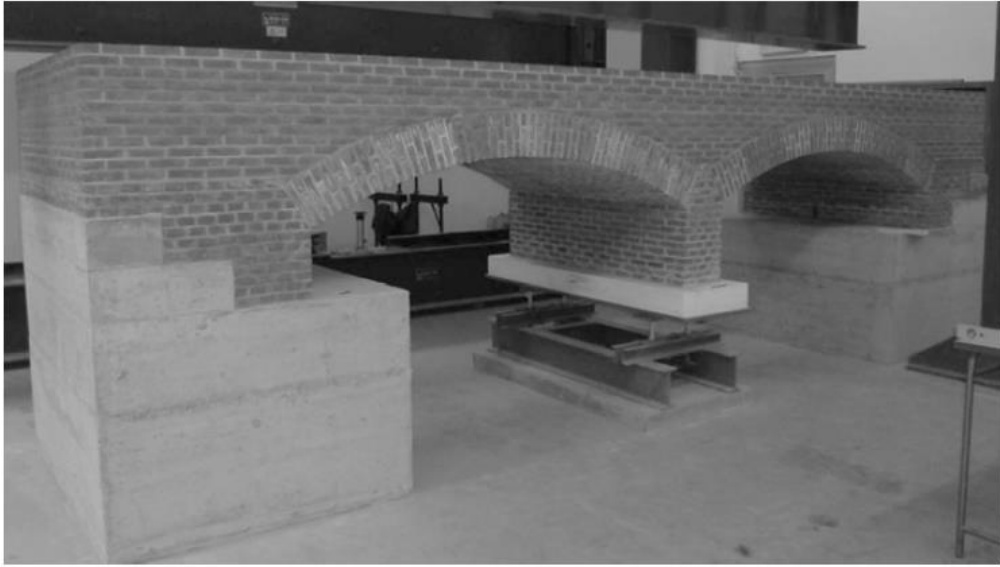


**Fig. 19** The scaled masonry bridge at Turin Polytechnic Lab. Clearly visible the settlement device under the central pier